INTRODUCTION

Roof fall accidents occur quite frequently at the intersections of underground openings and account for up to 30% of the roof fall fatalities (1,2). In the underground coal mines there are two types of entry intersections. One is four-way and the other is three-way intersections. At the intersection of two openings the maximum or diagonal roof span is wider than the width of each individual opening. This is considered to be one of the major reasons why roof falls occur more likely at the intersections than in the entry between pillars.

The most popular practices employed for roof support at intersections are to decrease roof bolt spacing 1 ft. less than or to increase roof bolt length 1 to 2 ft. longer than those employed in the entry between pillars (3). These practices seem to be adequate for some areas but in many cases inadequate for others.

A series of studies were therefore initiated to develop special techniques for intersection supports. In a previous paper, we proposed the preferable systems of bolting for the four-way entry intersections based on the three-dimensional stress analysis and field data. (4).

This report covers the study of three-way entry intersections. The three-dimensional finite element method was employed. Assuming that the bolt must be anchored in the rock strata outside the arching zone, the preferable systems of bolting were proposed. Also the amount of shear resistance required to inhibit sliding between layers was discussed.

Finite Element Model Analysis I
(Entries intersect at right angles)

2-1 The Model

The problem to be considered here is the analysis of a three-way entry intersection where entries intersect at right angles. A plane view of the right angle three-way intersection is shown in Fig 1. In the analysis entry widths varied at 14, 20 and 26 ft. Pillars which consist of coal were assumed to be 40 feet wide. Because of geometric symmetry, only the region, ABCD, was considered.

The idealized structural model of the region, ABCD, used in the finite element method is shown in Fig. 2. The model consists of rock and coal which were assumed to be linearly elastic, homogeneous and isotropic materials. The material properties used in the calculation are shown in Table 1. The coal seam of eight foot thick was assumed to be 592 ft. below surface.

The model was divided into 512 three-dimensional hexahedron elements each of which has eight nodes and 24 translational degrees of freedom. The model thus contained 729 nodal points and 2187 degrees of freedom. The computer program "NASTRAN" developed by NASA was used through out the analysis (5).

2-2 Results

The six components of stress and displacement dx, dy, dz, were obtained for each of the 512 elements. Since it is rather cumbersome to present all of the data, only those relevant to the subsequent analysis will be discussed here.

The vertical stress, σ_z, on the horizontal plane at midheight of the coal seam is shown in Fig. 3. The results indicate that for the 20 ft. entry intersection, the maximum vertical stress, σ_{max}, occurs at the corner of the

pillar. The results for the 14 and 26 ft. entry intersections show similar trends except the overall stress level is lower for the 14 ft. entry intersection while higher for the 26 ft. entry intersection. In Fig. 4 the maximum stresses of 3-way intersections are shown along with those of 4-way intersections. The maximum stresses of the 4-way intersections are consistently larger than those of the 3-way intersection and increase more rapidly with the width of the pillar.

Fig. 5 shows the vertical displacement, d, at the roofline of the 20 ft. entry intersection. In Fig. 6 the maximum displacements for the 14, 20 and 26 ft. entry intersections are shown together with those of the 4-way entry intersections. The maximum displacement of the 4-way intersections are consistently larger than those of the 3-way intersection and increase more rapidly with the width of the pillar.

The vertical stress at the roofline for 20 ft. entry is shown in Fig. 7. Tensile stress occurs at the intersection and along the centerline of the entry whereas compressive stress occurs along the ribs and increases toward the pillar. The areas where tensile stress occurs increase with the entry widths (Fig. 8). It is restricted to a small elliptical area at the intersection of the 14 ft. entry but expands along the axes of the entries as the entry width increases. The maximum tensile stresses at the intersections are shown in Fig. 9 (c) together with those at the 4-way entry intersections. The maximum tensile stresses at 3-way entry intersections are consistently larger than those at 4-way entry intersections. Also the maximum tensile stress at 3-way entry intersection increases rapidly as the entry width increases. The vertical stress contours on the vertical plane, BC, are shown in Fig. 10. A high stress concentration occurs near the rib of the pillar, the maximum value of which is found at the midheight of the pillar. A highly distressed zone appears above the intersection.

The horizontal stresses at the roofline are shown in Figs. 11 and 12. The maximum tensile stress in the x-direction appears above the corner of the pillar while the maximum in the y-direction appears near the centerline of the entry. The maximum tensile stress in the x-direction is larger than that in the Y-direction (Fig. 9). The maximum tensile stresses in both directions remain almost constants as the entry width increases, while those at the 4-way entry intersections show much change with the entry width.

Finite Element Model Analysis II
(Entries intersect at 30° and 60°)

3-1 The Model

A three-way entry intersections where entries intersect at 30 or 60 degrees were analyzed in this section. A plane view of the model used in the finite element analysis is shown in Fig. 13. The entries were assumed to be excavated in a coal seam having similar characteristics (i.e. seam depth, thickness) as assumed in the stress analysis of the 3-way rectangular intersection (Fig. 2). Also the same material properties in Table 1 were used.

The model was divided into 486 three-dimensional hexahedron elements with 700 nodal points.

3-2 The Results

The stress contours of the 30 and 60 degrees inclined entry intersections are shown in Figs. 14 and 15 where only the tensile stress contours are indicated.

The maximum tensile stresses in the vertical and x-directions occur near the centers of the intersections while the maximum tensile stress in

the y-direction occurs at the corner of the pillar with smaller angle. The maximum tensile stress in the verticle direction increases with decrease of inclination angle. The maximum tensile stress in the 30° inclined intersection is about twice of that in the rectangular intersection (Fig. 16). The maximum tensile stress in the y-direction also increases with decrease of inclination angle while the reverse is true for the stress in the x-direction. Assuming μ=1 and τ_o=0, the shear resistances, Sr, were calculated. The results show an increase in Sr with decreasing angle of inclination (Figure 16).

4. Proposed Roof Bolting Patterns
4-1 Suspension Method

There exists a highly destressed zone above the intersection as indicated by the calculated results. In the previous paper (4) it was found that the vertical stress contour line of $\sigma_z=0.1\sigma_o$ contours to the arch shape formed by the averaged roof falls at 4-way entry intersections. The contour line, $\sigma_z=0.1\sigma_o$ is considered to define the boundaries of the arch zone above the intersection that has more or less loosened up and requires supports. In the following sections the concept of arch zone defined by contour line, $\sigma_z=0.1\sigma_o$ is applied to the 3-way intersections.

If the strata within the arch zones discussed break and require immediate supports, the roof bolt patterns should be designed to carry the rock weight in this region. The idea is to suspend the broken rock to the overlying intact main roof outside the arch zone.

Fig. 17 indicates a typical pattern of the arching zone for the 20 ft. wide entry. Assuming that at least one extra foot of the bolts must be anchored at the strata outside the arch zone, the bolting patterns are proposed in Figs. 18, 19, and 20. For each case the area is divided into three regions,

I, II, III. For example, the region I of the rectangular intersection requires a bolt length egual to or longer than 40% of the entry width. The carrying weight per unit area in this region is then 0.4 ρ_RgWe, where ρ_Rg is the weight per unit volume of the strata. The region II and III of the rectangular intersection require a minimum bolt length of 0.3 and 0.2 We respectively as shown in Fig. 18. The bolting patterns proposed in Fig. 18 can be applied to the rectangular intersection when an entry-to-pillar width ratio, We/Wp is betweem 0.35 and 0.65. For the intersection with an entry-to-pillar width ratio less than 0.35 the bolting patterns might be applied while they give a more conservative bolt design.

The 60-degree-inclined intersection does not show an apparent increase of the minimum required bolt lengths as compared with those of the rectangular intersection while the 30-degree inclined intersection required about 25% to 50% more bolt lengths.

4-2 Friction Reinforcement Method

If there are thinly laminated strata in the immediate roof, roof bolting patterns should also be designed to strengthen these strata. This can be achieved by clamping them together to become a combined thick beam. A combined thick beam deflects or sags less than the combined result of separated thin strata. The principle behind the beam building is to increase the interstrata shear resistance which reduces or prohibits interstrata sliding.

The shear resistance, Sr, required to prevent sliding between strata may be calculated by the following equations:

$$\begin{aligned} &\text{if } \sigma_z > 0, \quad Sr = \tau_r - \mu\sigma_z - \tau_o \\ &\text{if } \sigma_z < 0, \quad Sr = \tau_r - \tau_o \end{aligned} \tag{7}$$

where $\tau r = \sqrt{\tau xz^2 + \tau yz^2}$, μ is the coefficient of friction and τo is the cohesive shear strength between strata. If the assuptions that μ =1 and τo=0 are made for Eq. 7, the shear resistances required to prevent slidings between strata are calculated. The most critical area is located on the line a-b in Fig. 21 in a horizontal plane approximately 0.15 We above the roofline. The zone where shear resistance is required, that is, Sr > 0 prevails up to 0.28 We above the roof line. The required shear resistance for a retangular 3-way entry intersection does not show signficant change with the widths of entry in contrast with the one for 4-way entry intersection.

In Figs. 22, 23, and 24, the proposed bolting patterns for rectangular, 60-degree-inclined and 30-degree-inclined intersections are shown. The required bolt lengths, shear resistances and pretensions are combined in Table 2 where the following assumption that a pretension of

$$P = (\tau r - u0z - \tau o)/\mu \qquad (8)$$

is required to prevent the sliding between the strata is made.

In the reinforcement method the required bolt lengths are proportional to the entry widths and increase when the coefficient of friction, μ, declines. The required capacity or strength is highly dependent on the coefficiant of friction, cohesive shear strength and insitu stress before excavation. But in the suspension method the required anchorage capacity or strength and length of the bolt do not vary with them. Therefore in designing an optimum roof bolting patterns for an intersection, the required anchorage capacities or strengths and lengths of the bolt shall be calculated for both methods. A choice between the two methods can then be made based on the available anchorage capacity, bolt length, strata conditions and other requirements.

Conclusions

1. The calculated results indicate that an arching zone is formed above a three-way intersection and a region of vertical tensile stress is developed over a short distance into the roof.

2. The maximum tensile vertical stress and required shear resistance of a three way intersection are considerably larger than those of the four-way intersection of same entry width.

3. The tensile vertical stress and required shear resistance increases with decrease of angle of entry inclination. Thus the 30-degrees-inclined intersection is hardest to support among the cases examined.

4. Suspension and reinforce methods of roof supports were studied. Preferable bolting systems for both methods were proposed in the paper.

REFERENCES

1. Dougherty, J.J. "A Study of Fatal Roof Fall Accidents in Bituminous Coal Mines", M.S. E.M. Thesis, West Virginia University, Morgantown, WV, 1971, 77 pps.

2. Van Bisien, A.C., "Analysis of Roof Fall Accident Statistics and Its Application to Roof Control Research", Paper presented at AIME Annual Meeting, Chicago, Ill., Feb. 28-March 1, 1973, Preprint No-73-F-71, 11 pps.

3. Stahl, R.W., "Survey of Practices in Controlling Roof at Intersections and Junctions in Underground Coal Mines", IC 8133, 1962, 13 pps.

4. Peng, S.S. and Okubo, S., "Roof Bolting Patterns at the Four-way Entry Intersections", Paper presented at AIME Annual Meeting. Denver, Colorado, Feb. 28-March 2, 1978, Preprint No. 78-AM-5.

5. McCormick, C.W. (Ed.), "The NASTRAN User's Manual", (Level 15.0), National Aeronautics and Space Administration, Washington, D.C., 1973.

TABLE 1. Properties of Rock and Coal

Material	Young's Modulus kp/ft^2	Poisson's Ratio	Specific Gravity
Rock	1.83×10^5	0.25	2.5
Coal	0.55×10^5	0.30	1.3

TABLE 2. Required Length and Strength of a Bolting Pattern.

	μ	Rectangular	60 Degrees Inclined	30 Degrees Inclined
l_b (Ft.)	0.8	0.4 We	0.4 We	0.4 We
	1	0.3 We	0.3 We	0.3 We
	1.2	0.2 We	0.2 We	0.2 We
Sr (psi)	0.8	$0.16\sigma_o - \tau_o$	$0.19\sigma_o - \tau_o$	$0.25\sigma_o - \tau_o$
	1	$0.15\sigma_o - \tau_o$	$0.12\sigma_o - \tau_o$	$0.16\sigma_o - \tau_o$
	1.2	$0.07\sigma_o - \tau_o$	$0.08\sigma_o - \tau_o$	$0.11\sigma_o - \tau_o$
P (psi)	0.8	$0.2\sigma_o - \tau_o$	$0.24\sigma_o - \tau_o$	$0.32\sigma_o - \tau_o$
	1	$0.1\sigma_o - \tau_o$	$0.12\sigma_o - \tau_o$	$0.16\sigma_o - \tau_o$
	1.2	$0.06\sigma_o - \tau_o$	$0.07\sigma_o - \tau_o$	$0.1\sigma_o - \tau_o$

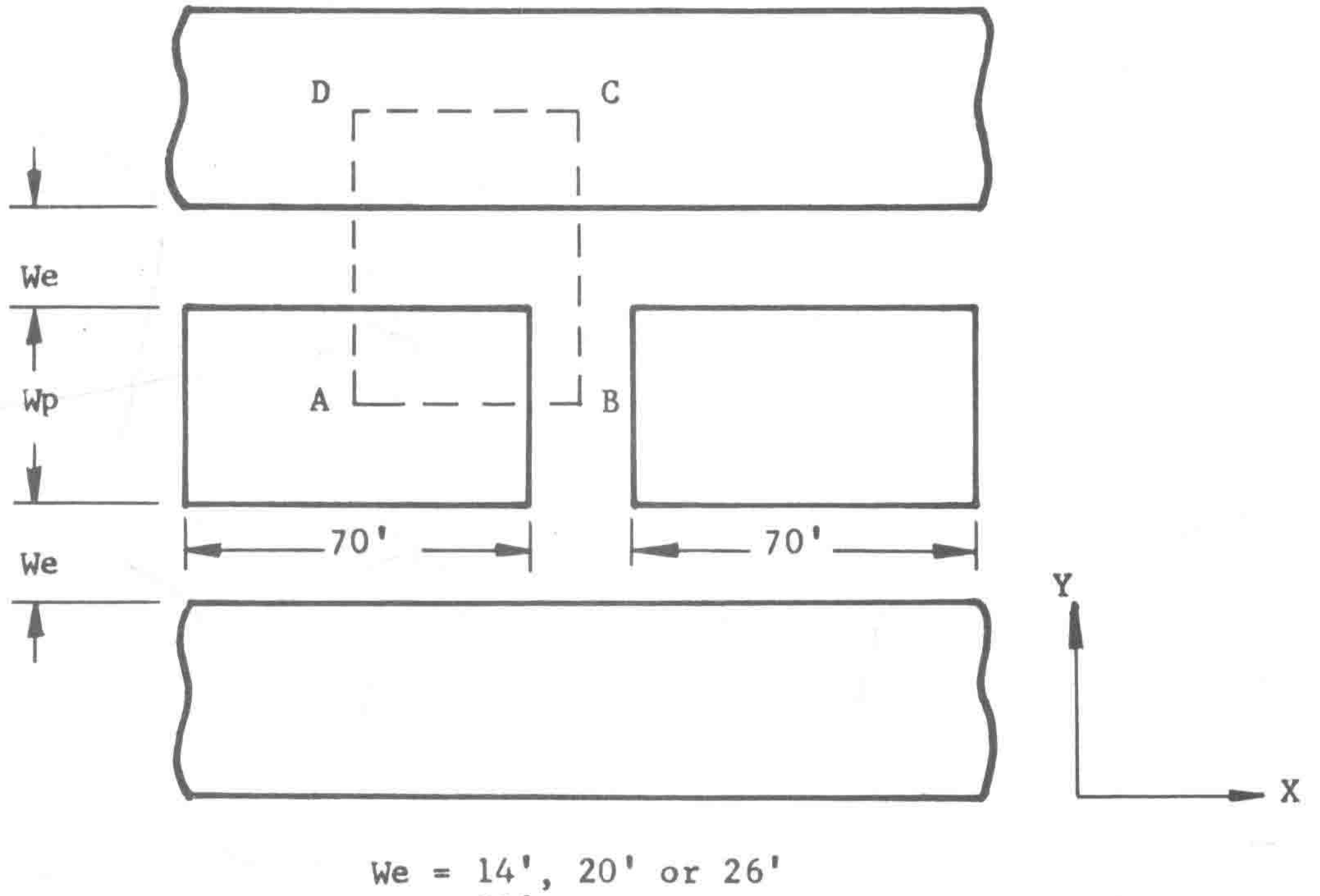

We = 14', 20' or 26'
Wp = 40'

Fig. 1 Horizontal Plane View of 3-Way Intersection

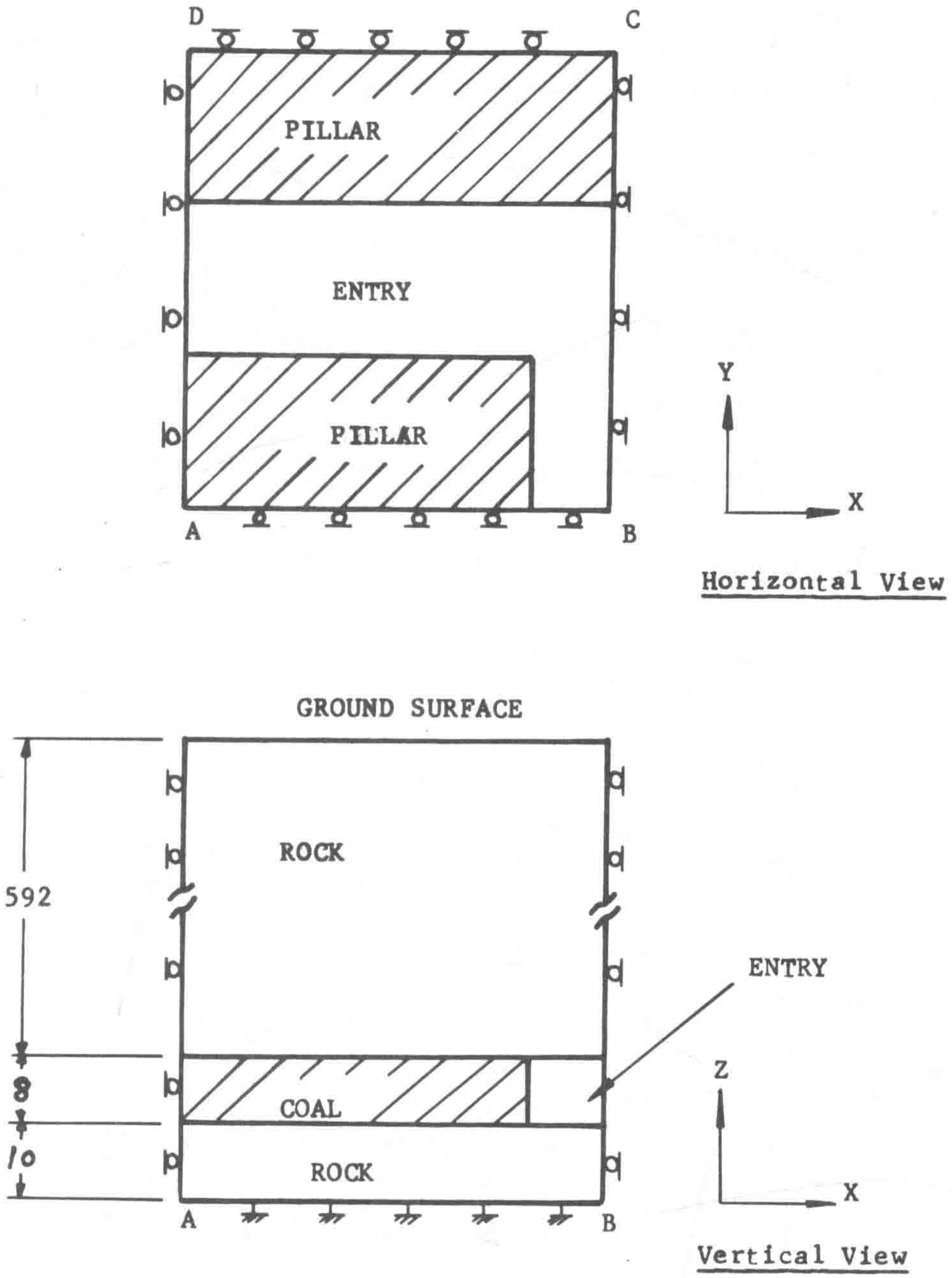

Fig. 2 The Finite Element Model of the Right Angle 3-Way Intersection

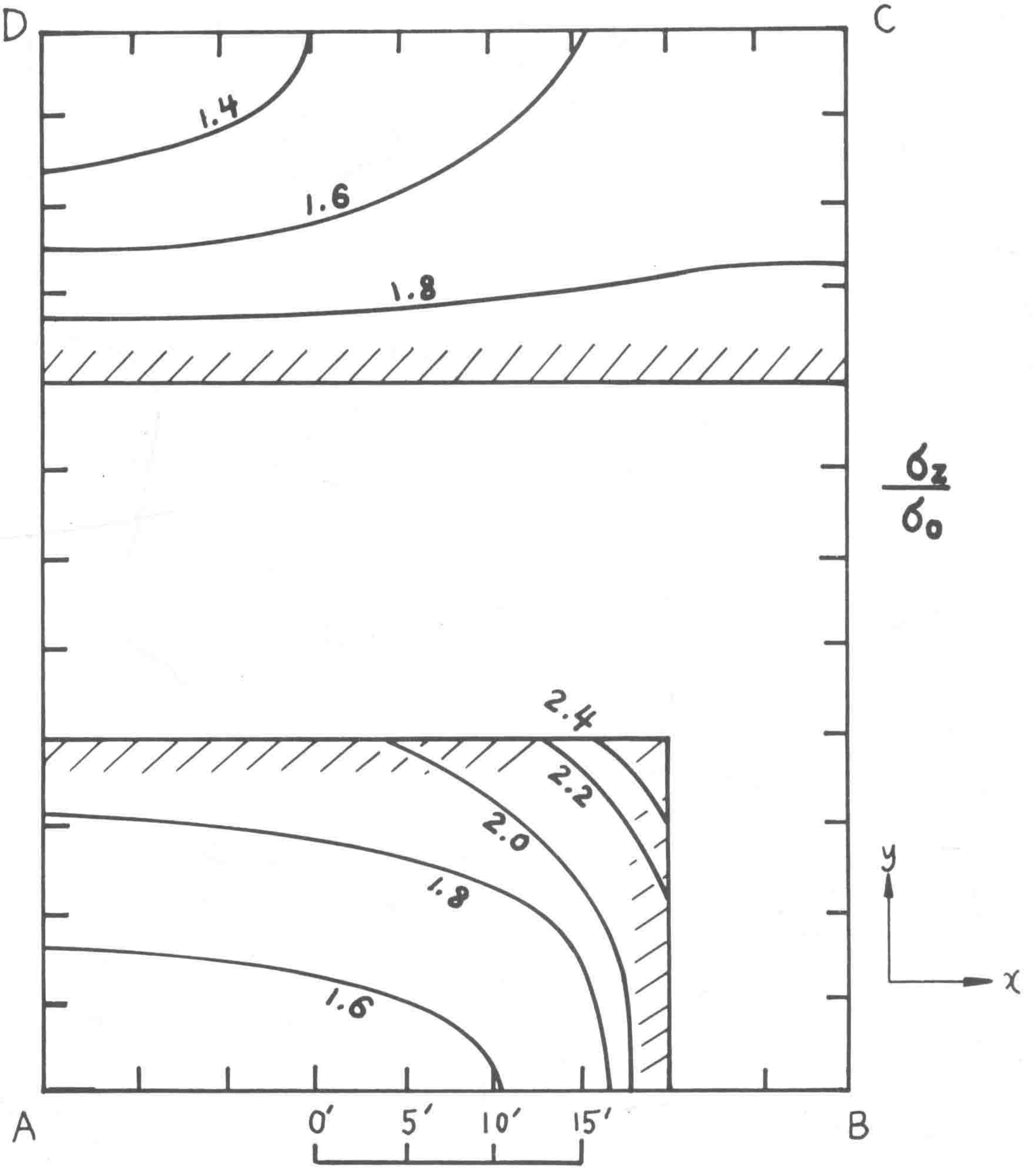

Fig. 3 Vertical Stress Distribution at Mid-height of Coal Seam - 20 Ft. Entry Intersection

$\therefore \sigma_o$ = overburden stress .

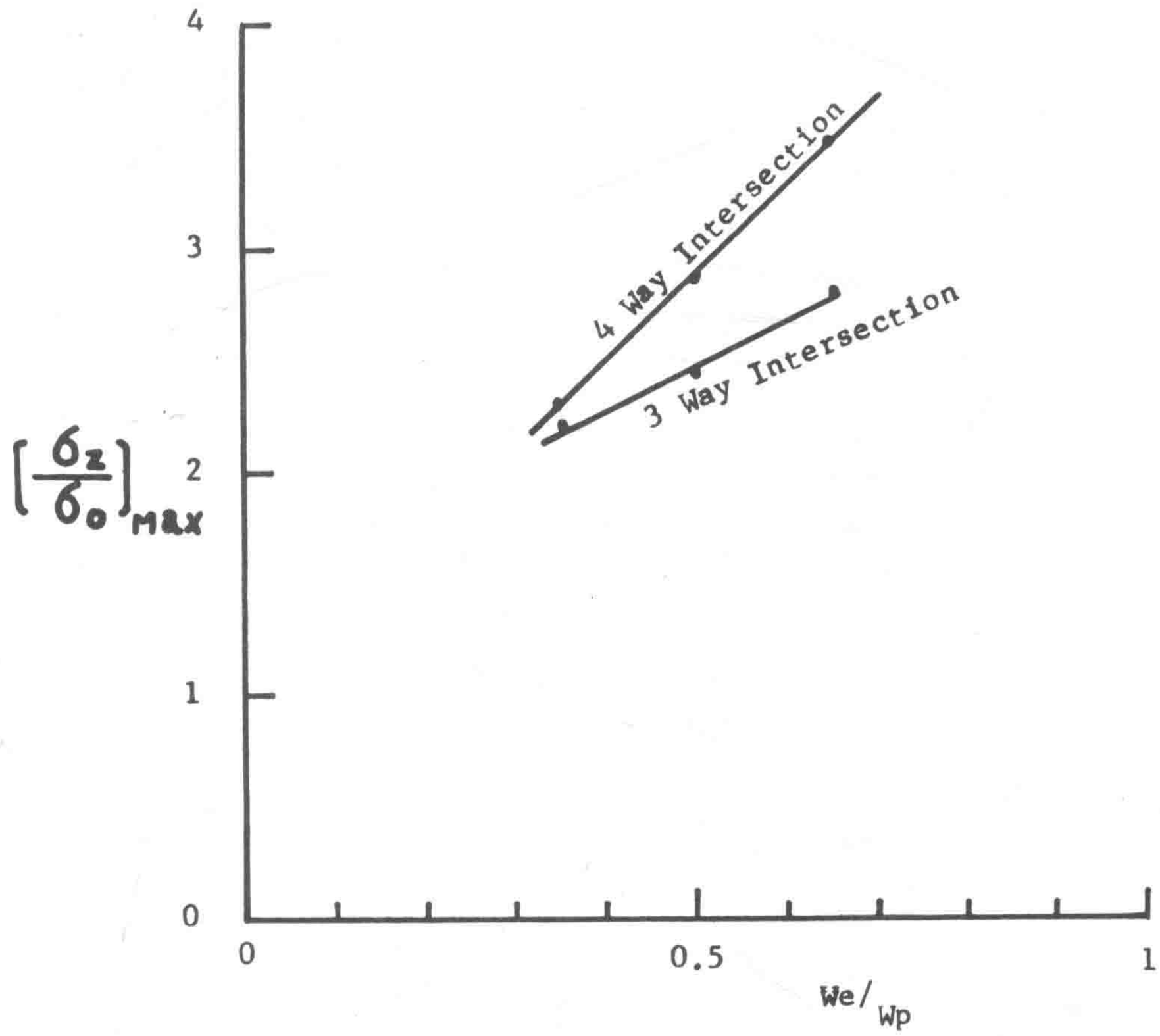

Fig. 4 Maximum Vertical Stresses in the Pillars

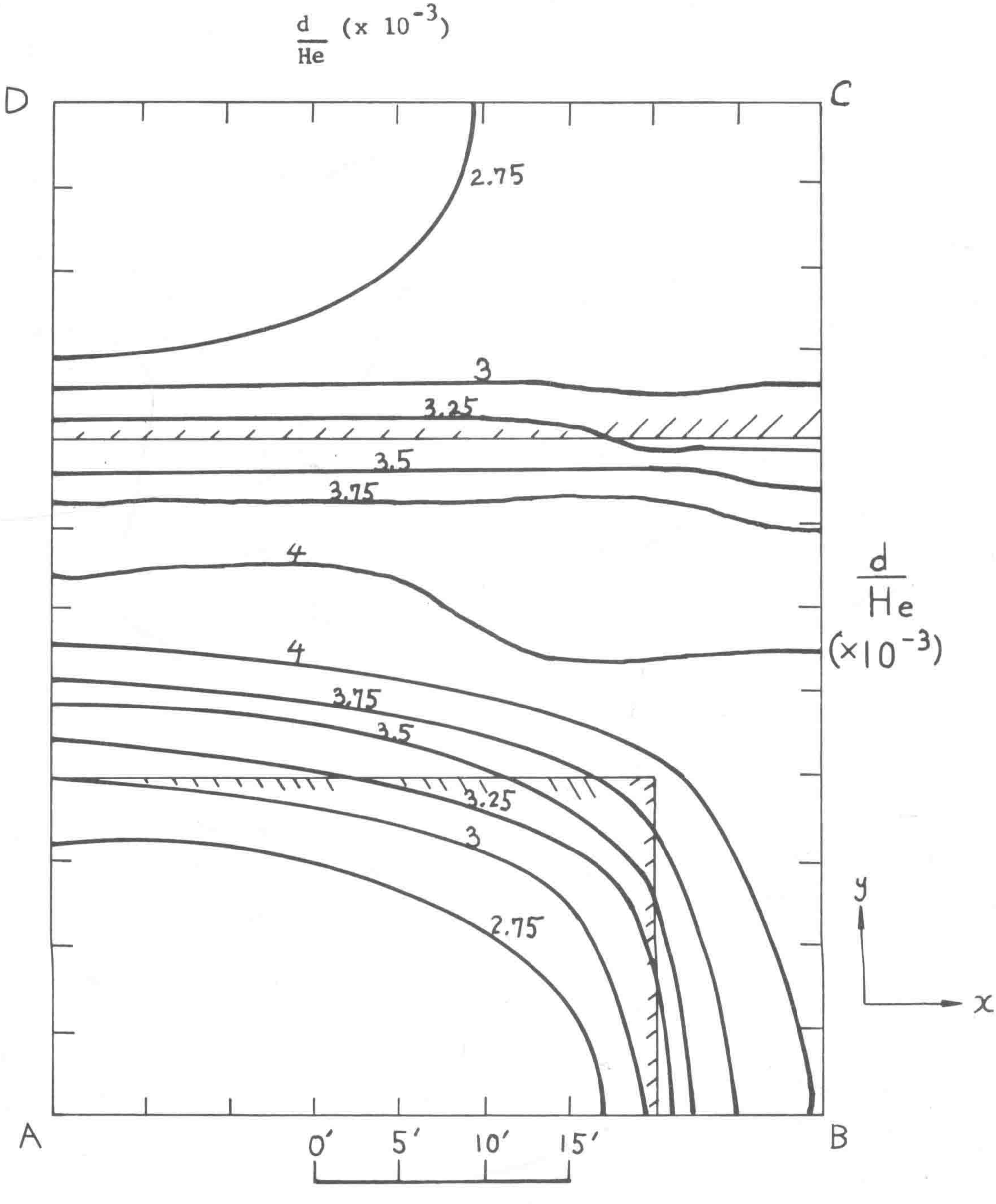

We = 20', He = 8' (Height of Entry)

Fig. 5 Vertical Displacement of Roof Plane - 20 Ft. Entry Intersection

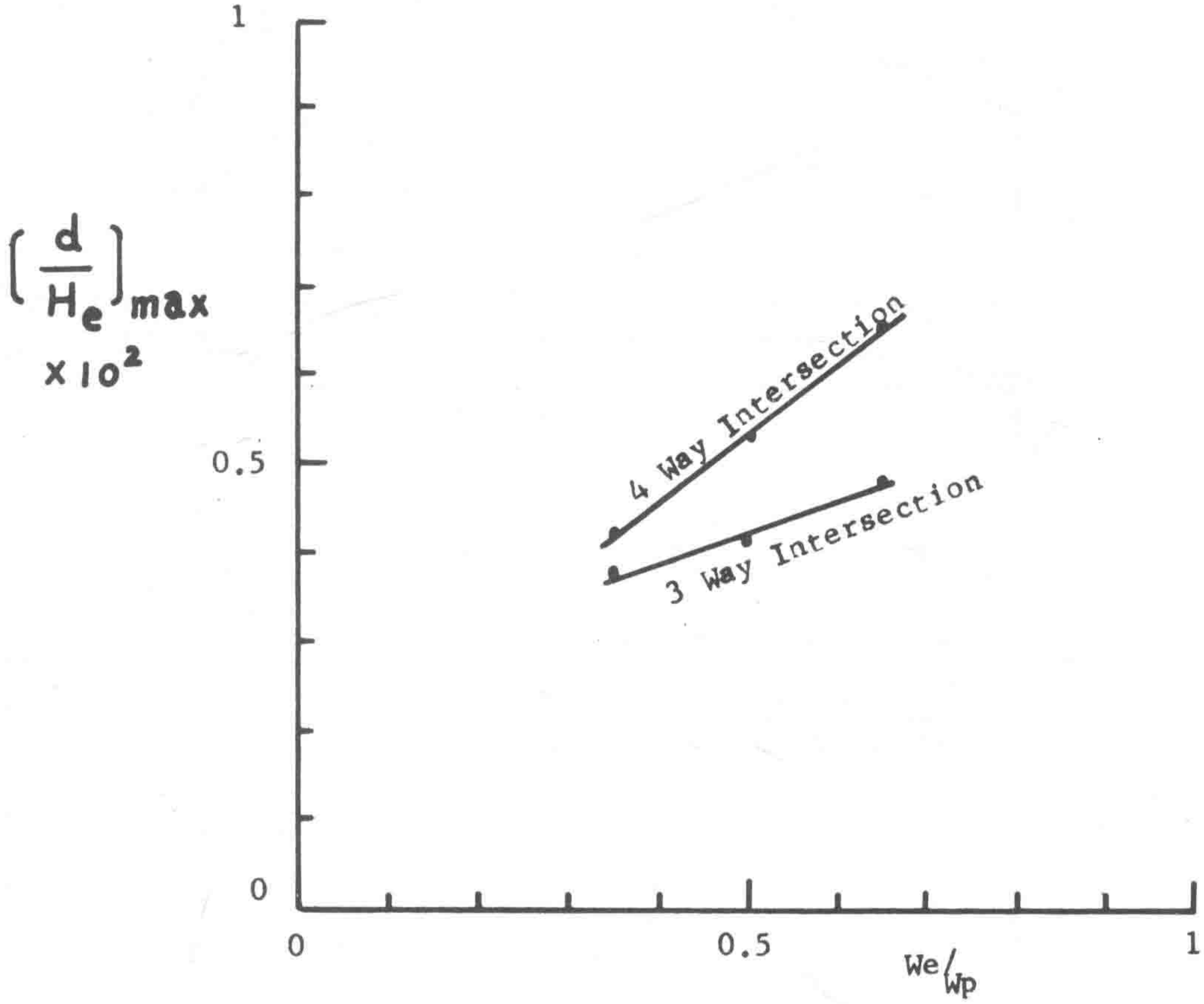

Fig. 6 **Maximum Vertical Displacement of the Roof Plane**

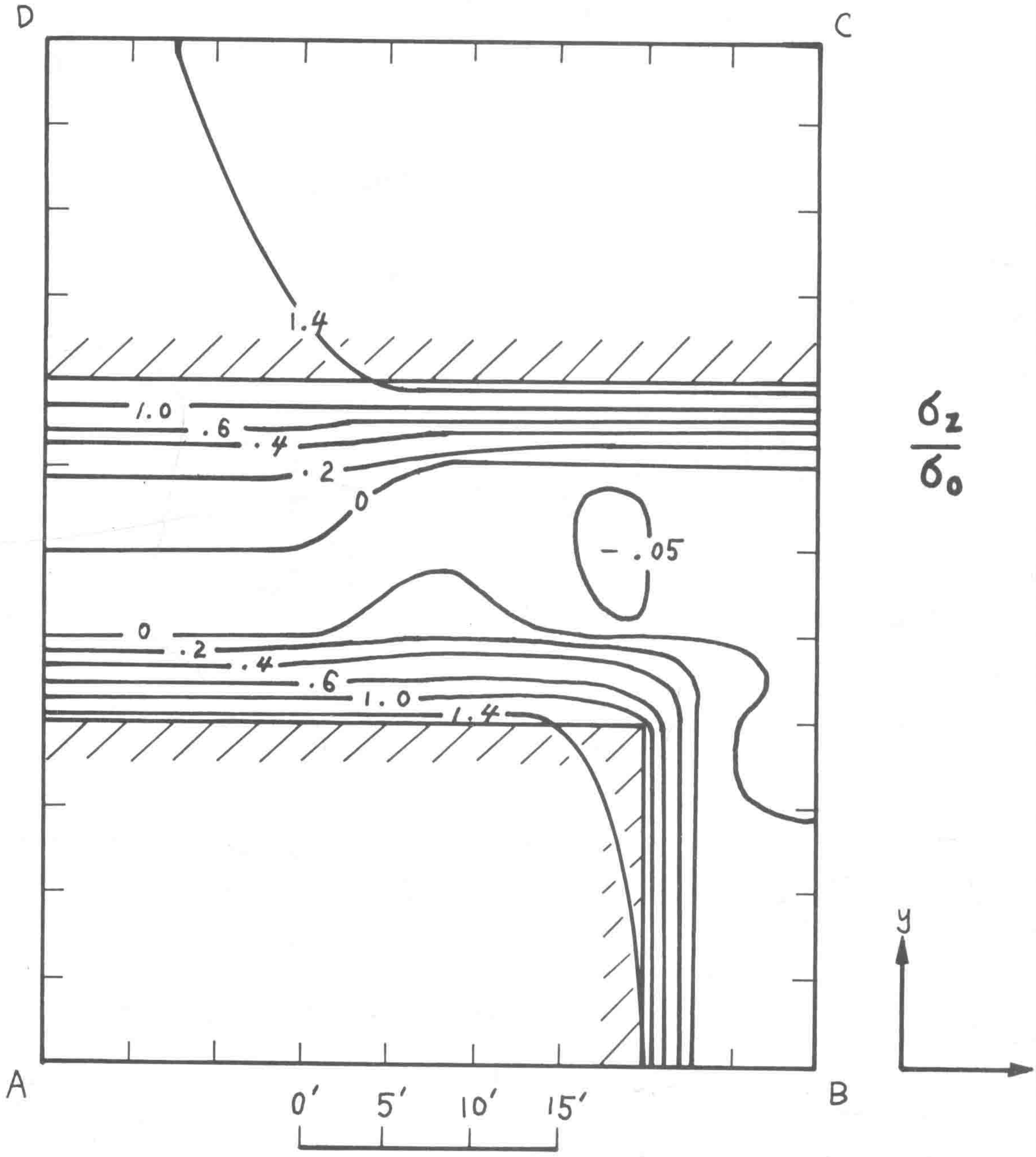

$\frac{\sigma_z}{\sigma_o}$

Fig. 7 Vertical Stress Contour of 1 Ft. Above the Roof Plane - 20 Ft. Entry Intersection

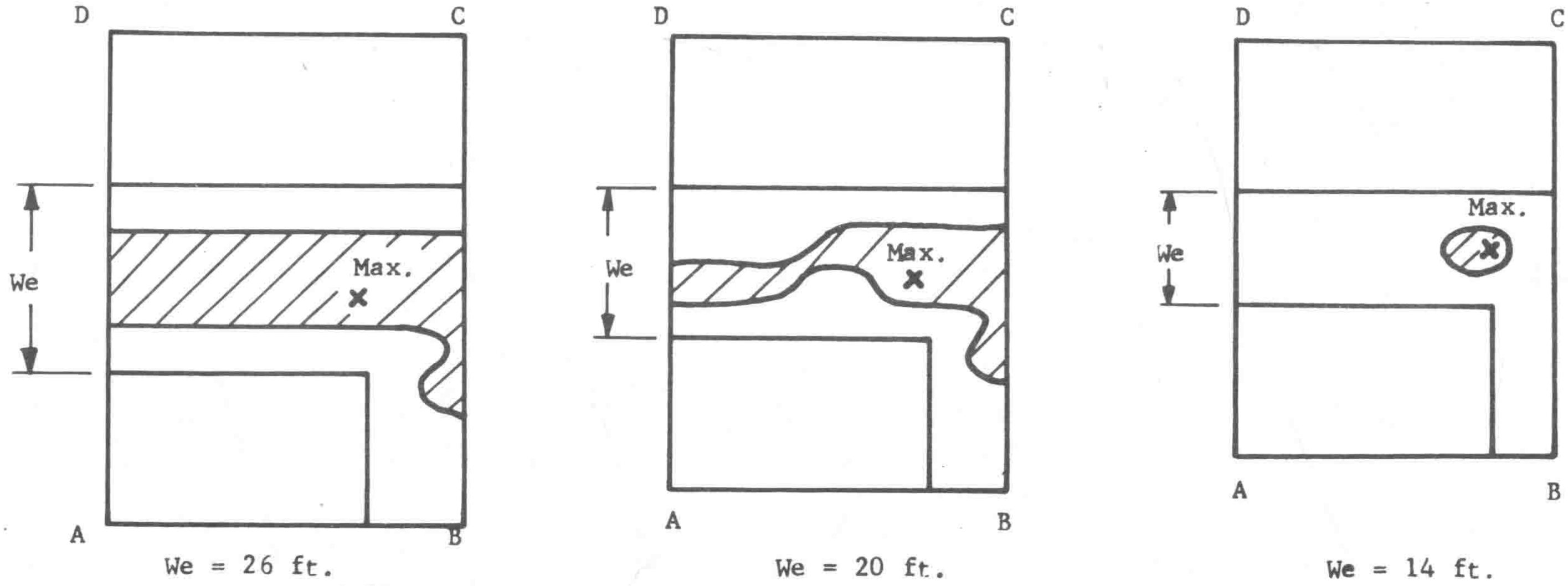

Fig. 8 Tensile Stress Zone at 1 Ft. Above the Roof Plane at Entry Intersections

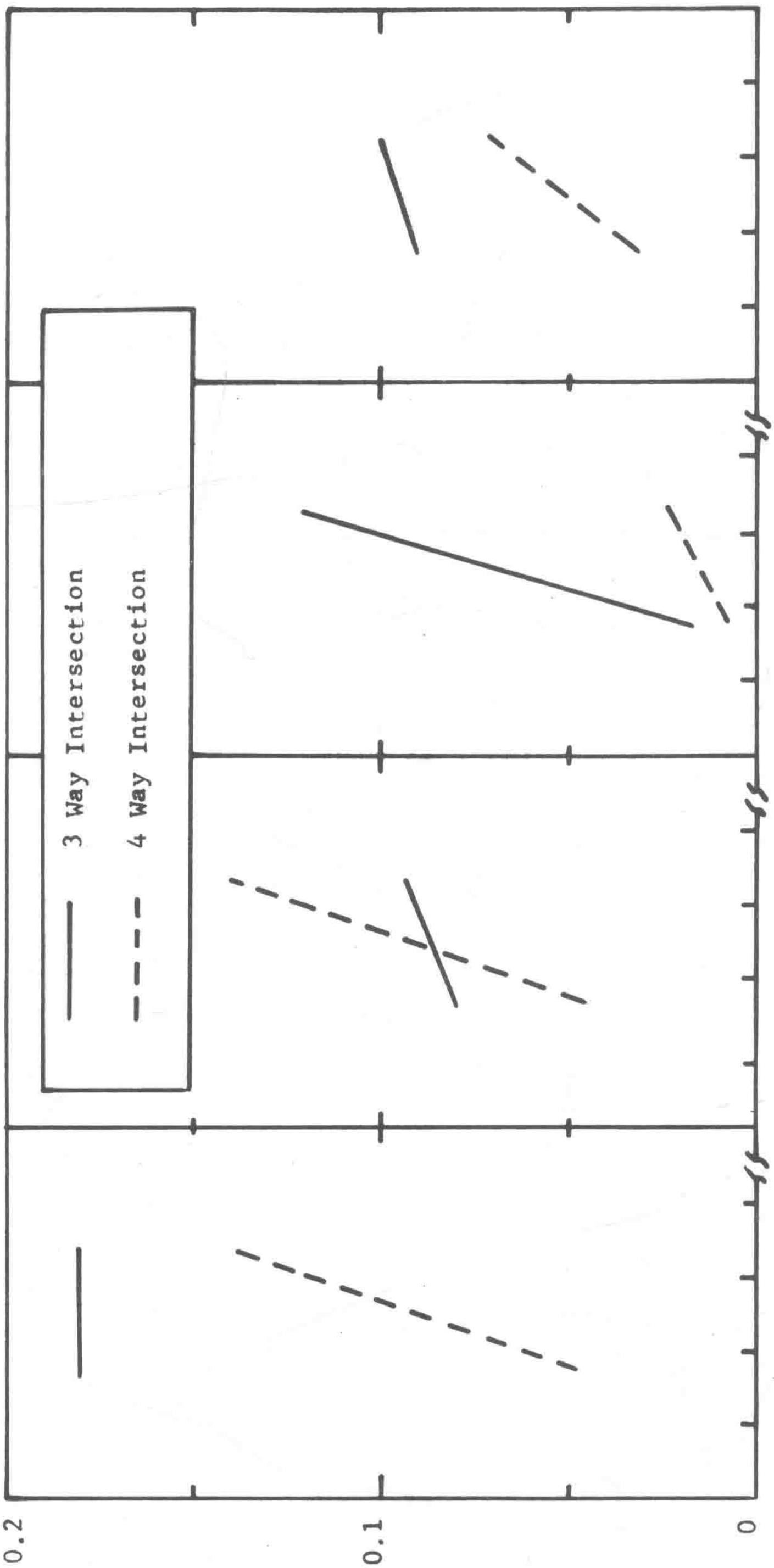

Fig. 9 Max. Stresses in the 3-Way and 4-Way Entry Intersections

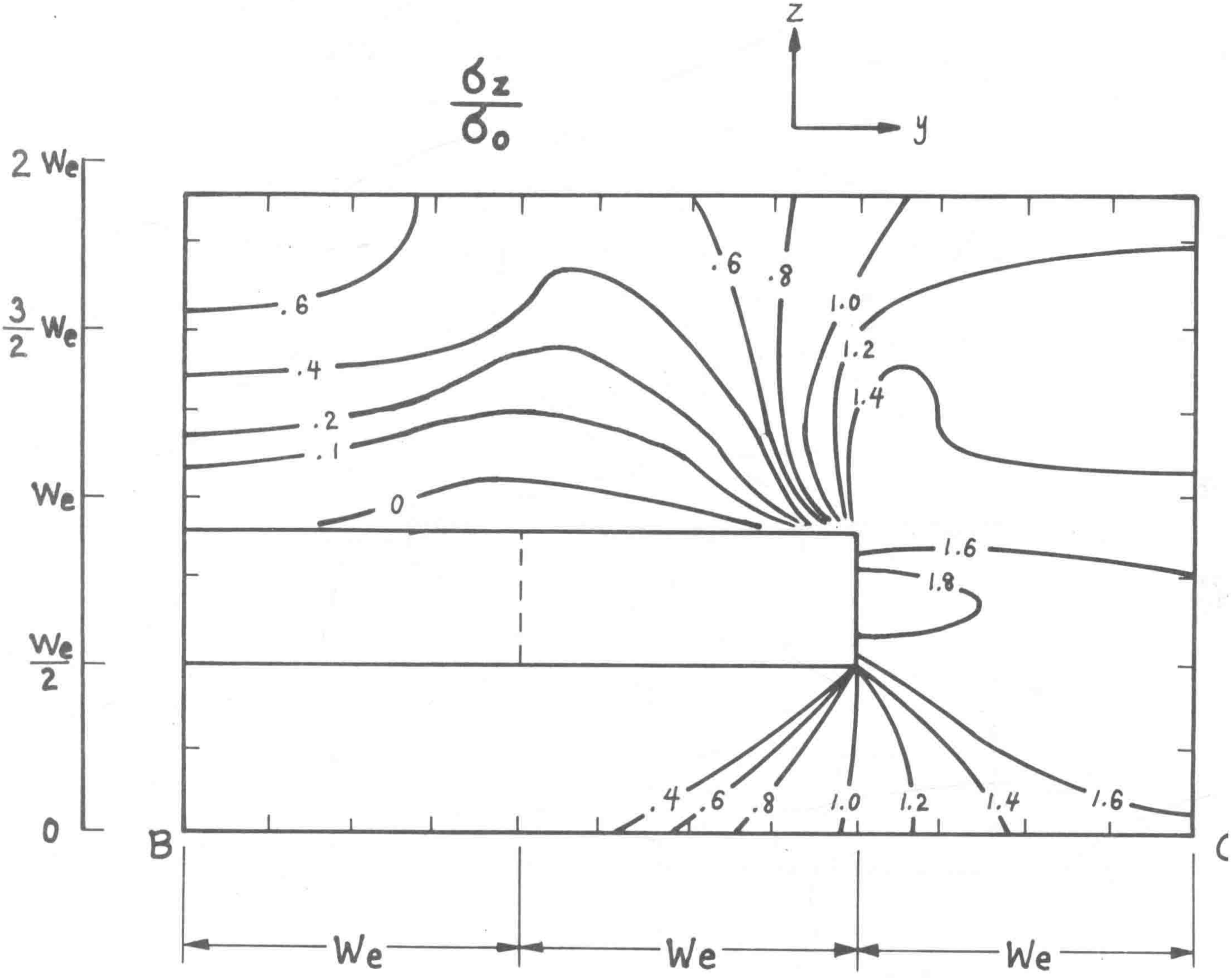

Fig. 10 Contour of Vertical Stress on Vertical Plane B - C - 20 Ft. Entry Intersection

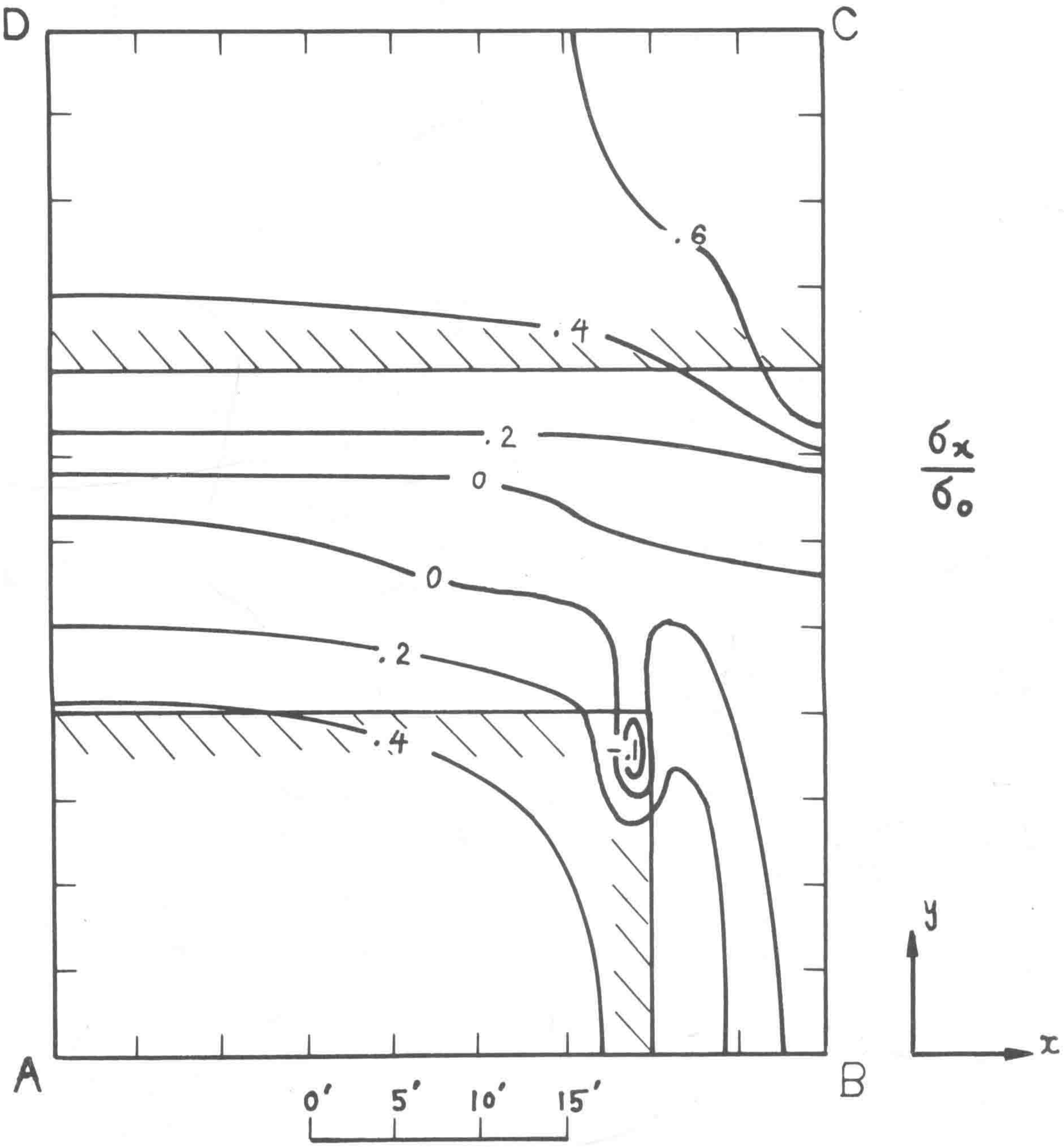

Fig. 11 Horizontal Stress, σx at 1 Ft. Above the Roof Plane - 20 Ft. Entry Intersection

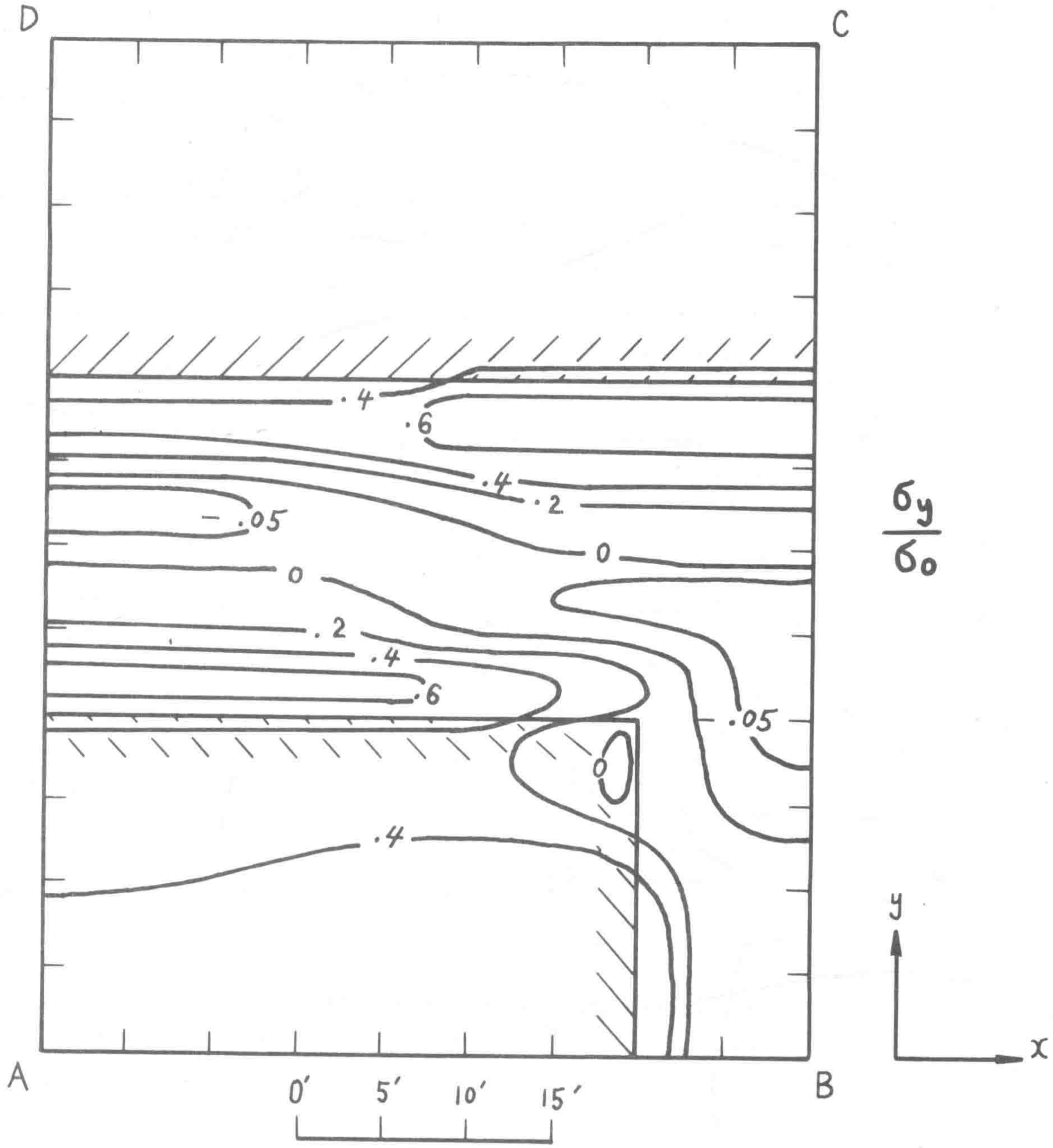

Fig. 12 Horizontal Stress, σ_y at 1 Ft. Above the Roof Plane - 20 Ft. Entry Intersection

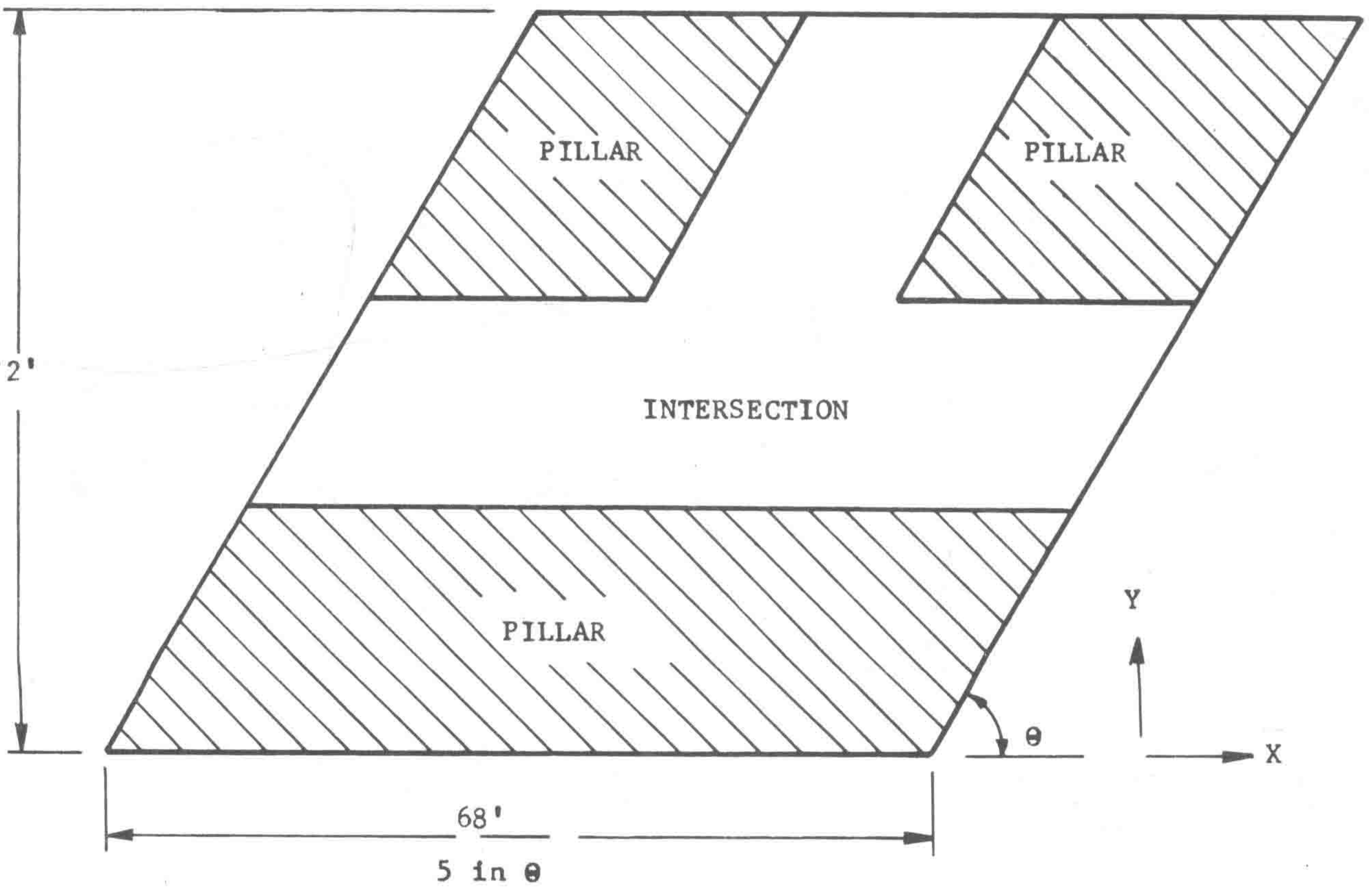

Fig. 13 The Finite Element Model of the Inclined 3-Way Intersections

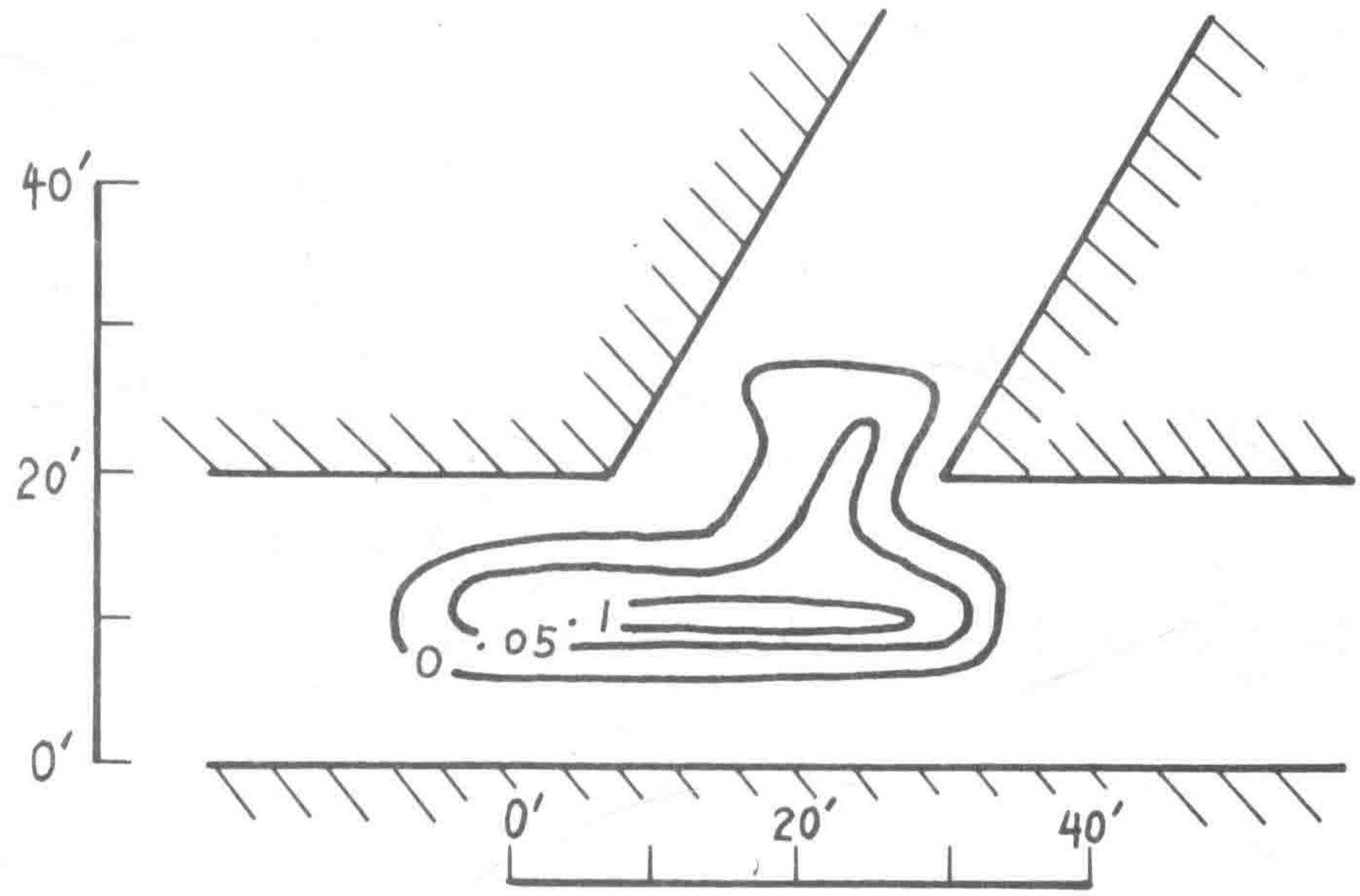

(a) $-\frac{\sigma_z}{\sigma_o}$

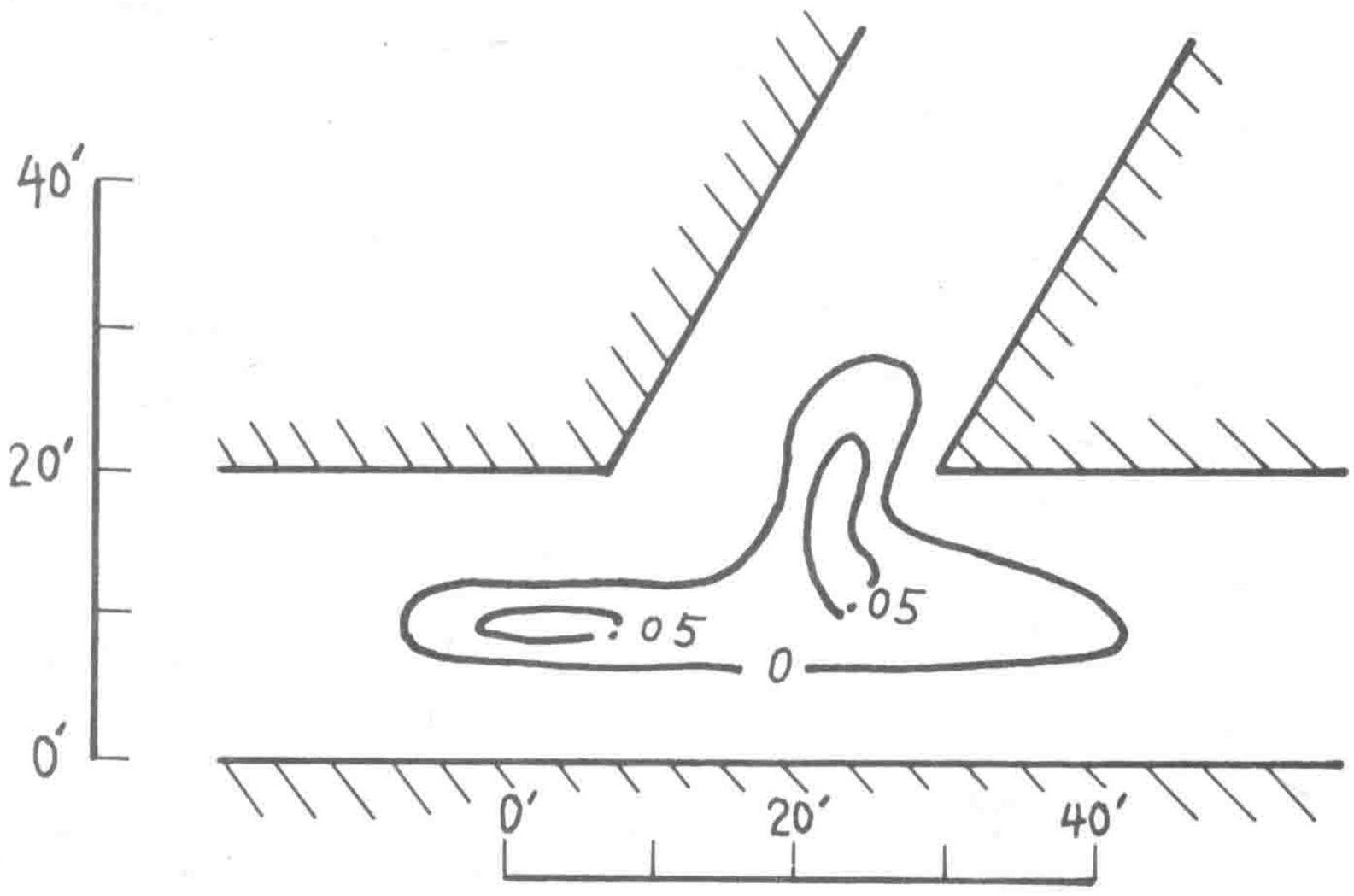

(b) $-\frac{\sigma_x}{\sigma_o}$

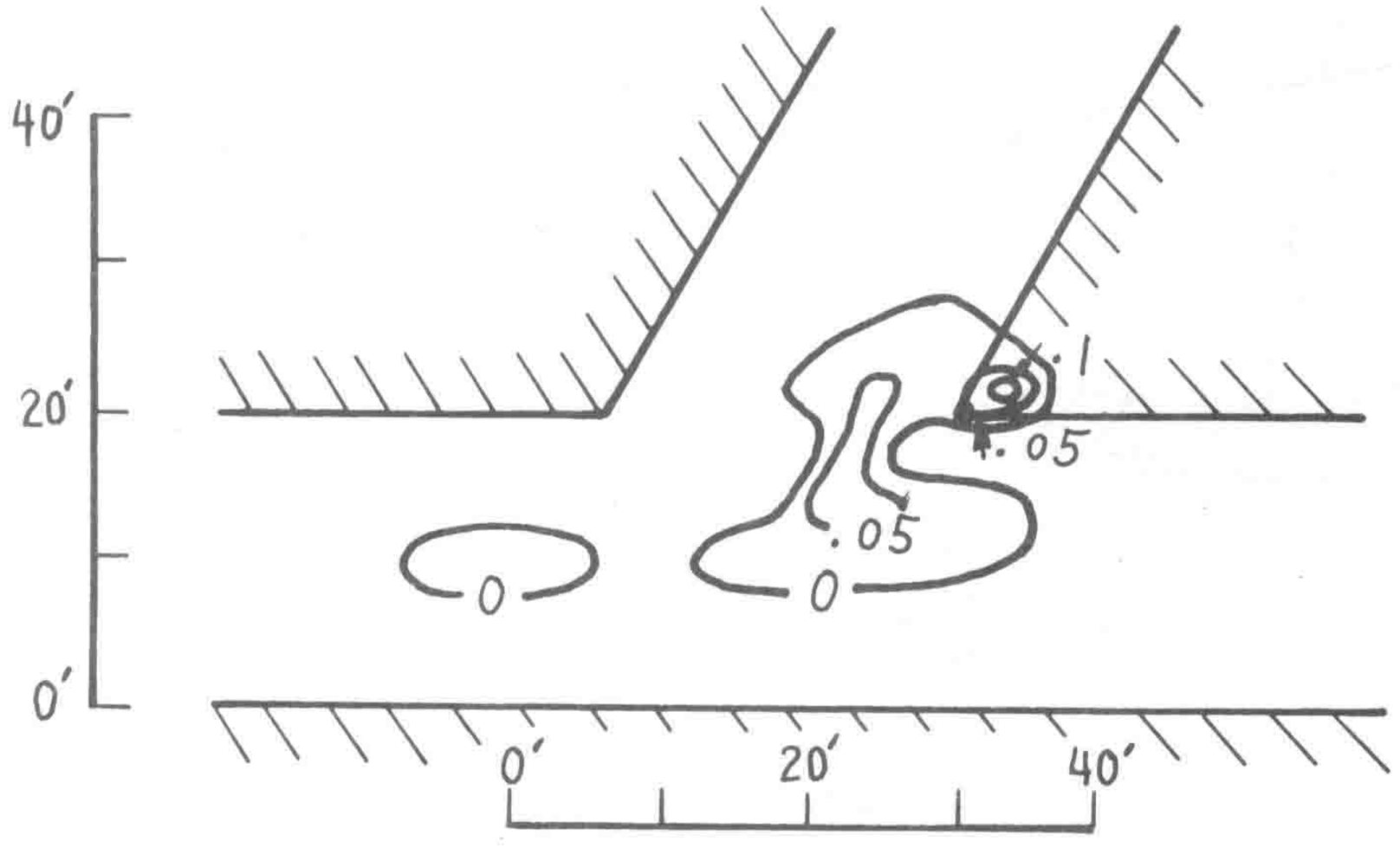

(c) $-\frac{\sigma_y}{\sigma_o}$

Fig. 14 Stress Contours at 1 Ft. Above the Roof Line - 60 Degrees Inclined, 20 Ft. Entry Intersection

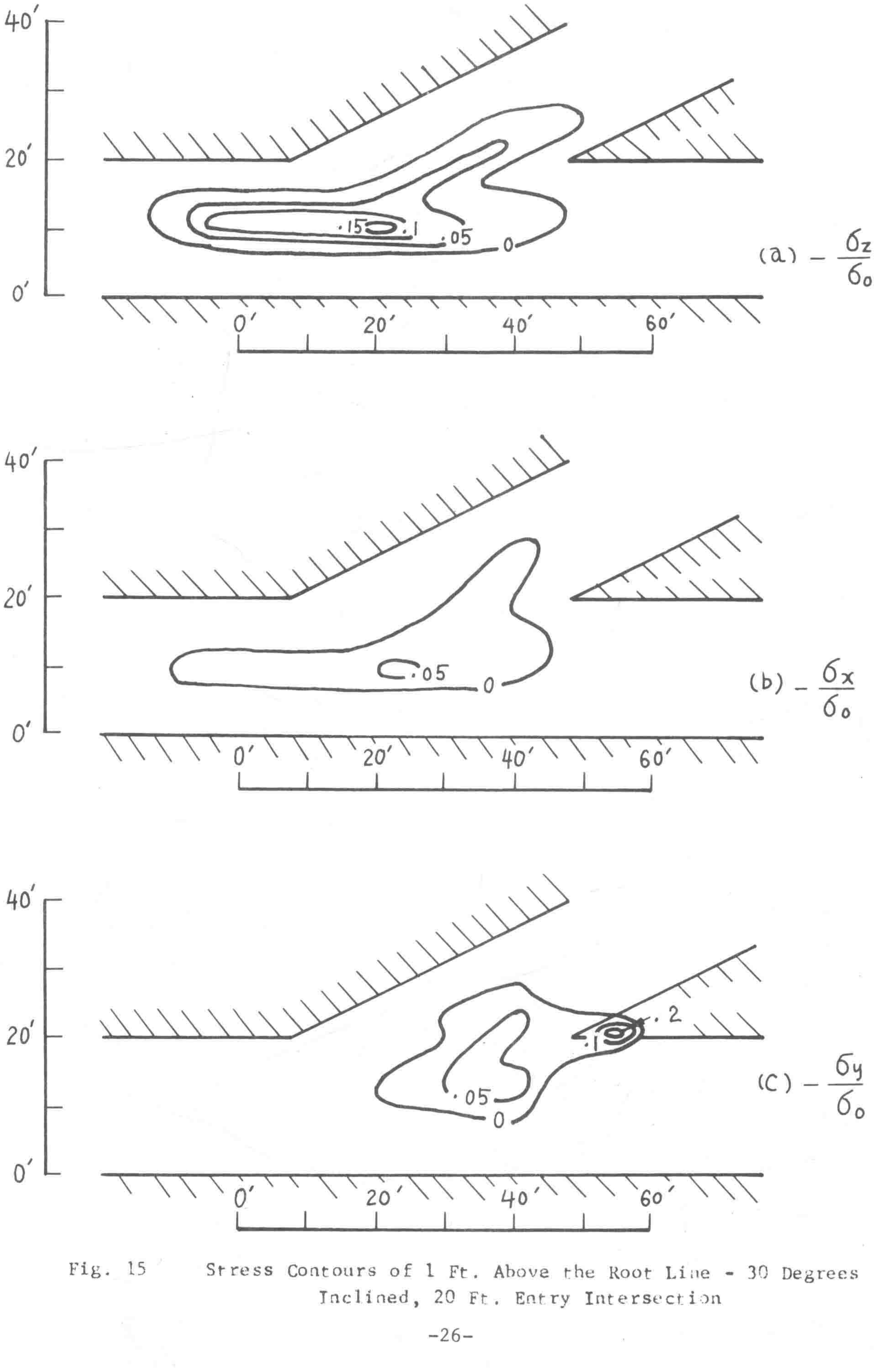

Fig. 15 Stress Contours of 1 Ft. Above the Root Line - 30 Degrees Inclined, 20 Ft. Entry Intersection

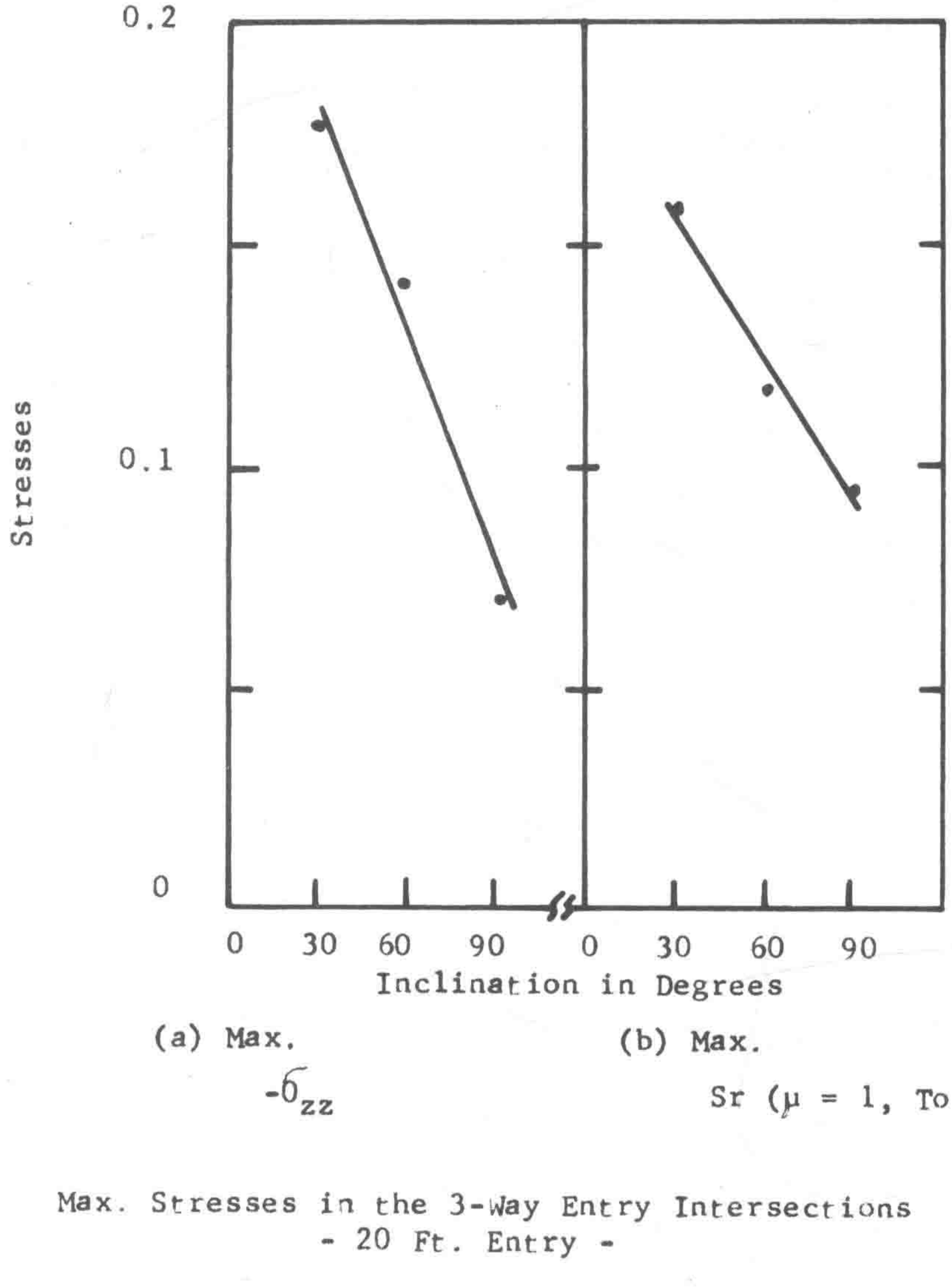

Fig. 16 Max. Stresses in the 3-Way Entry Intersections
- 20 Ft. Entry -

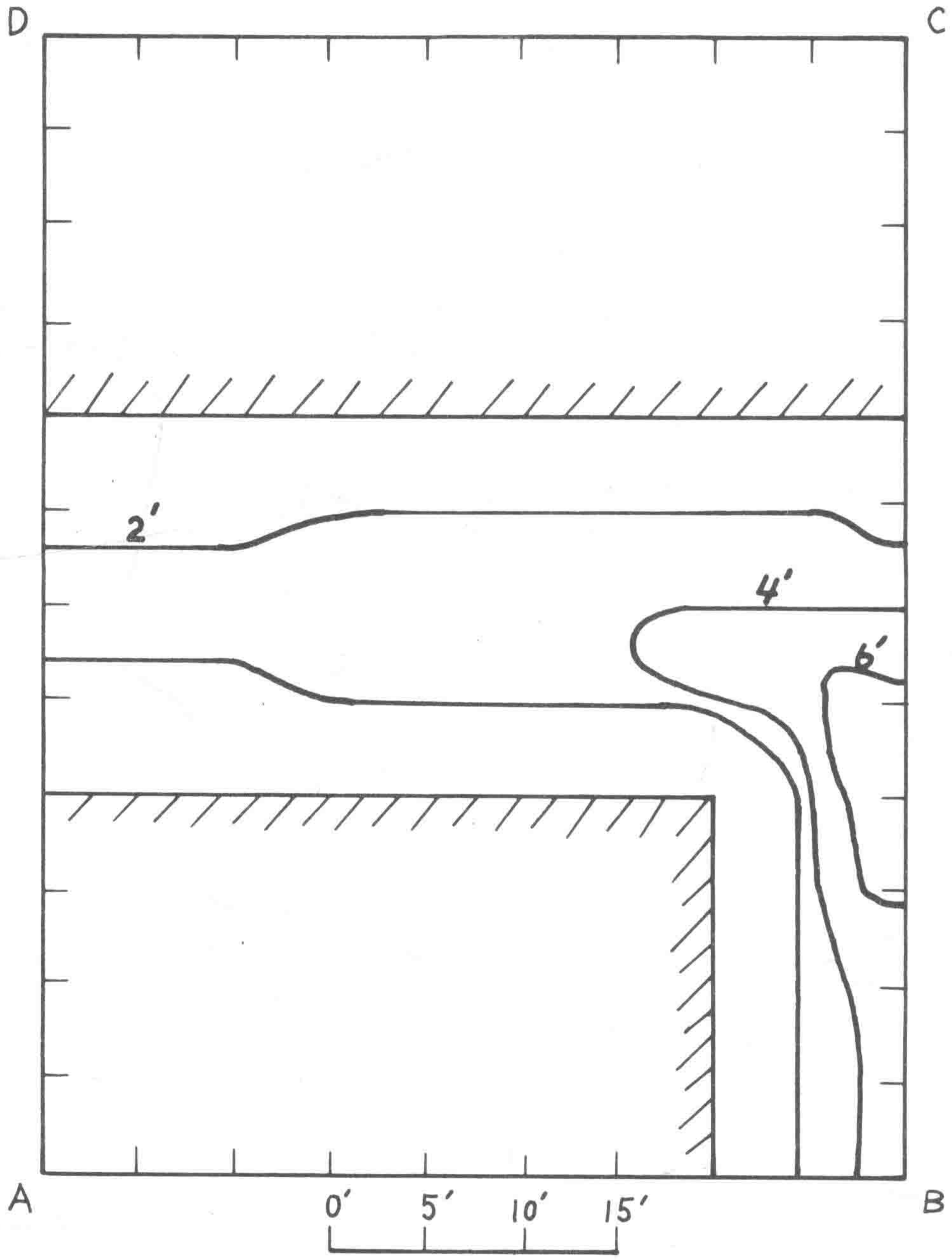

Fig. 17 Height of the Arching Zone Measured From the Roof Plane - 20 Ft. Entry Intersection

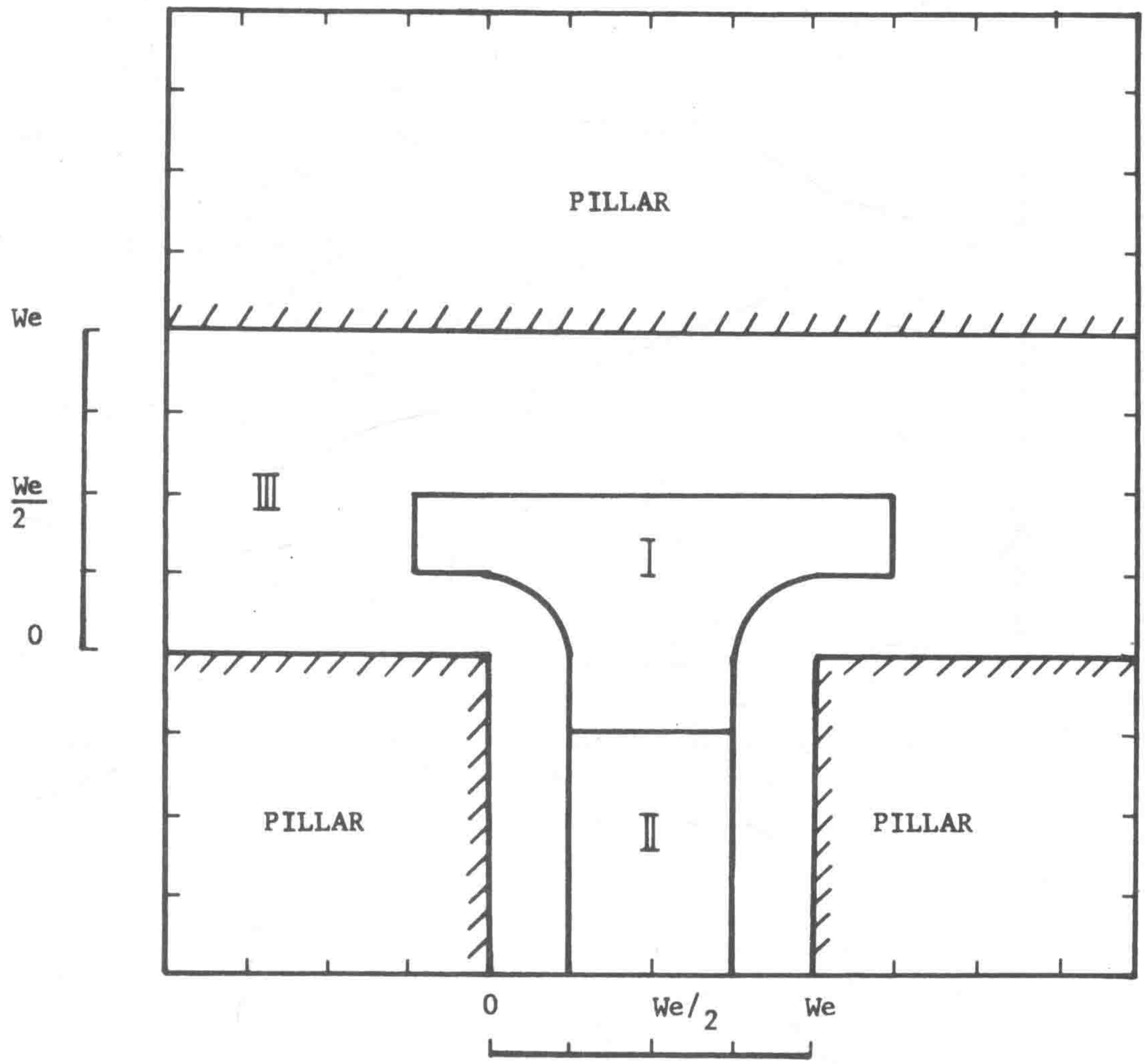

REGION	BOLT LENGTH	CARRING CAPACITY
I	0.4 We	0.4 ρ_R g We
II	0.3 We	0.3 ρ_R g We
III	0.2 We	0.2 ρ_R g We

Fig. 18 The Proposed Bolting Pattern for Suspension Method

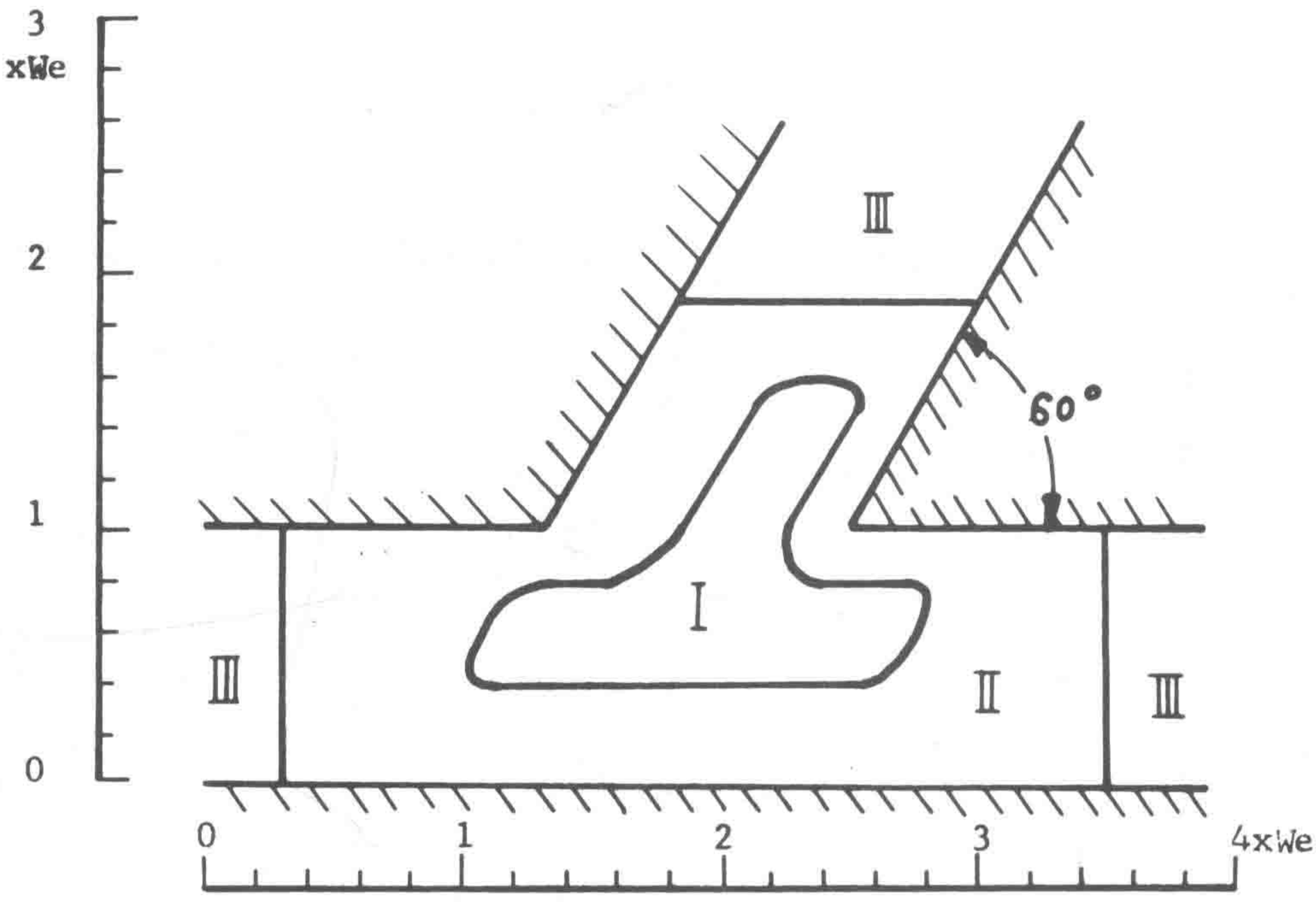

REGION	BOLT LENGTH	CARRING CAPACITY
I	0.4 We	0.4 ρ_R g We
II	0.2 We	0.2 ρ_R g We
III	0.15 We	0.15 ρ_R g We

Fig. 19 The Proposed Bolting Pattern for Suspension Method

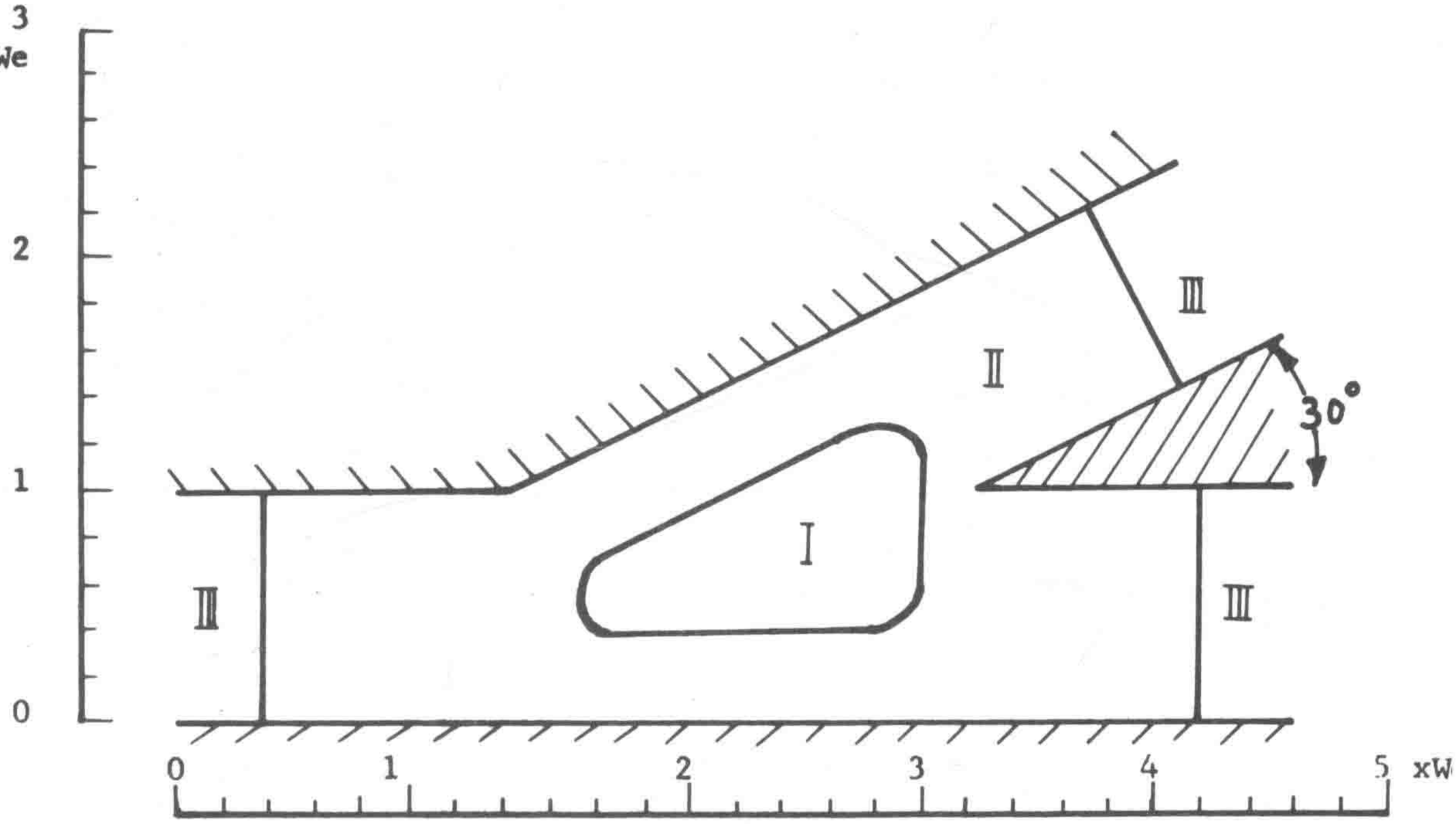

REGION	BOLT LENGTH	CARRING CAPACITY
I	0.5 We	0.5 $\rho_R g$ We
II	0.3 We	0.2 $\rho_R g$ We
III	0.15 We	0.5 $\rho_R g$ We

Fig. 20 The Proposed Bolting Pattern for Suspension Method

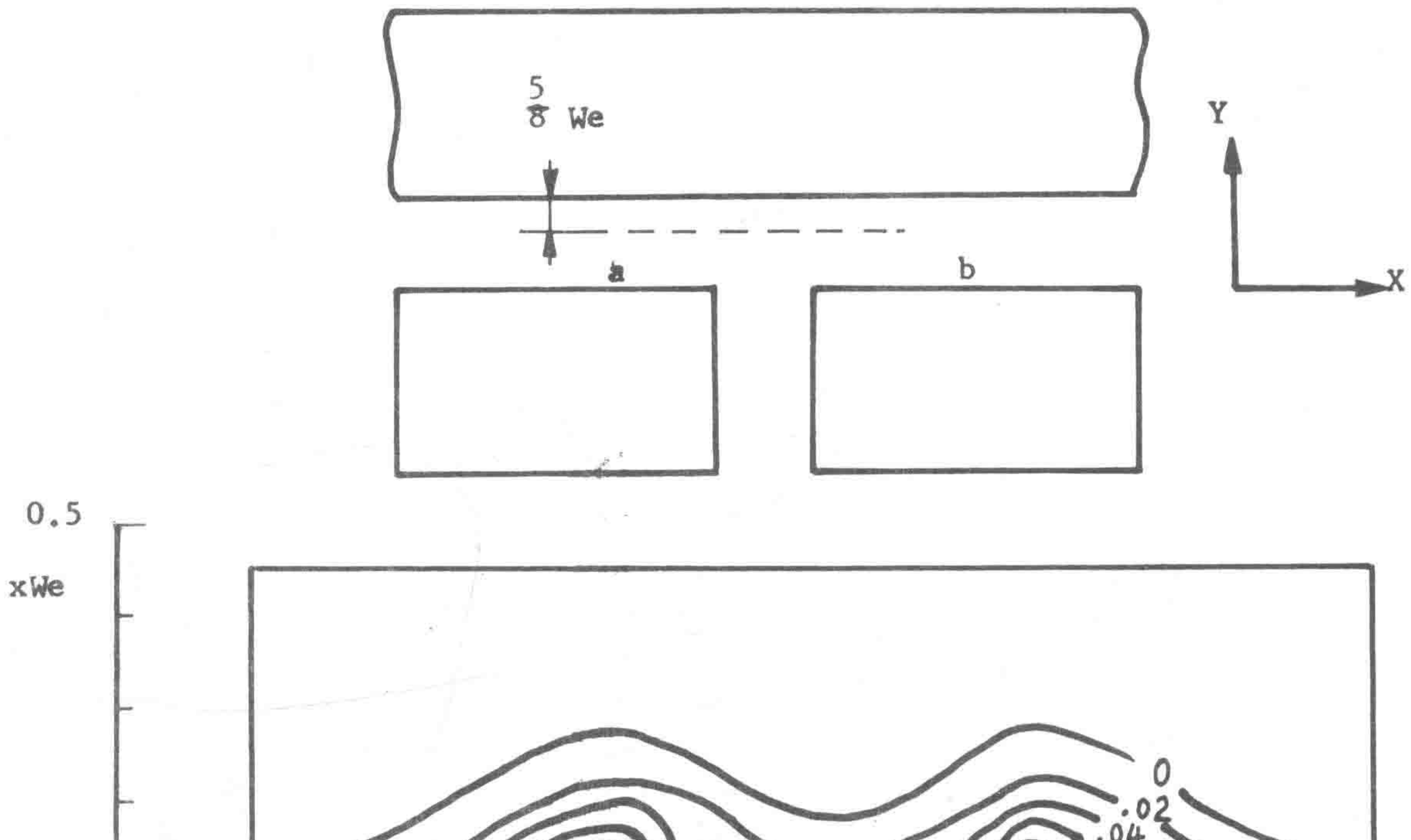

Fig. 21 Distribution of Sliding Stress on the Vertical Plane

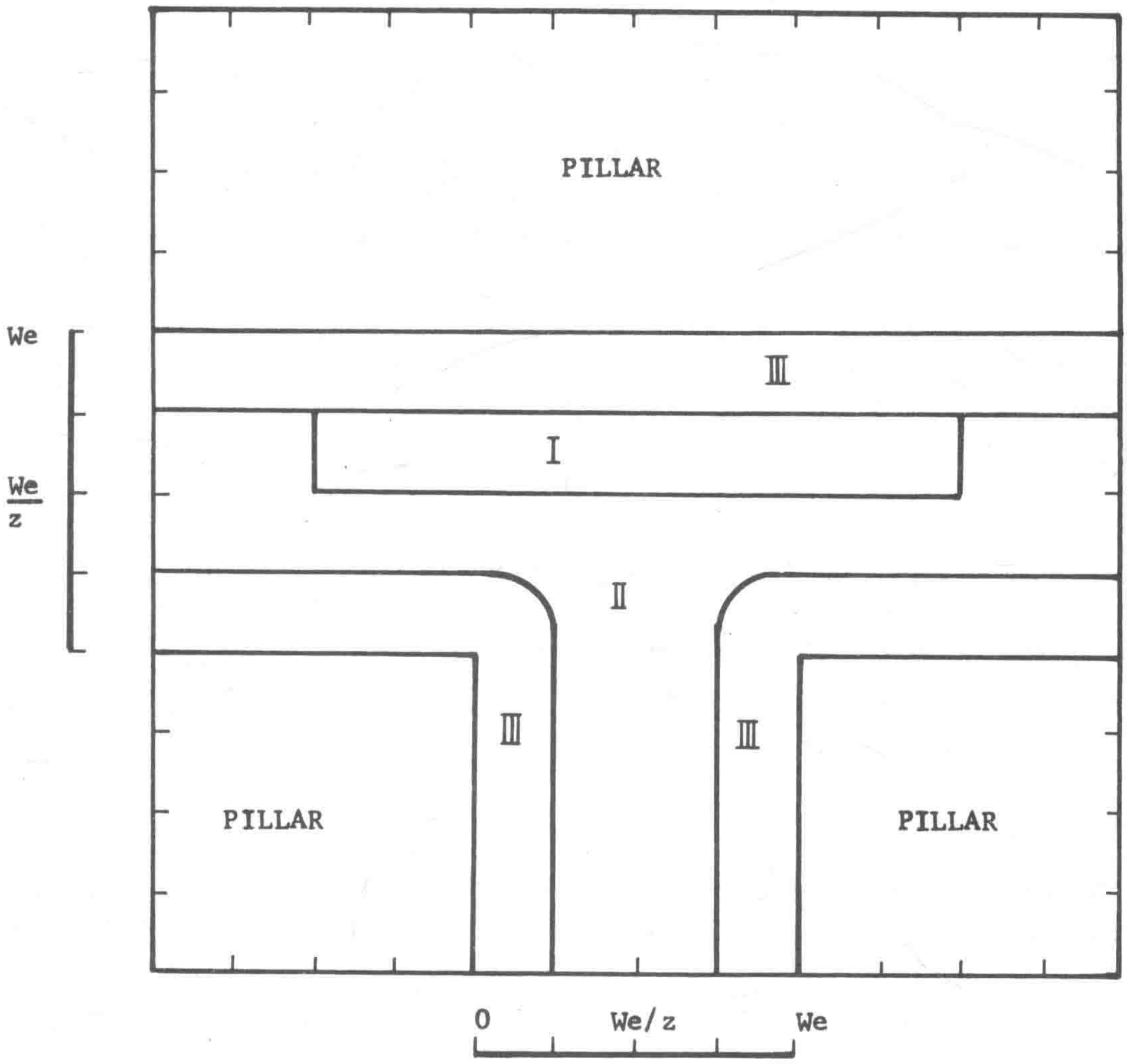

REGION	BOLT LENGTH	REQUIRED SHEAR RESISTANCE	REQUIRED PRETENSION
I	l_b	Sr	P
II	0.8 l_b	0.5 Sr	0.5 P
III	0.6 l_b	0.3 Sr	0.3 P

Fig. 22 The Proposed Belting Pattern for Reinforcement Method

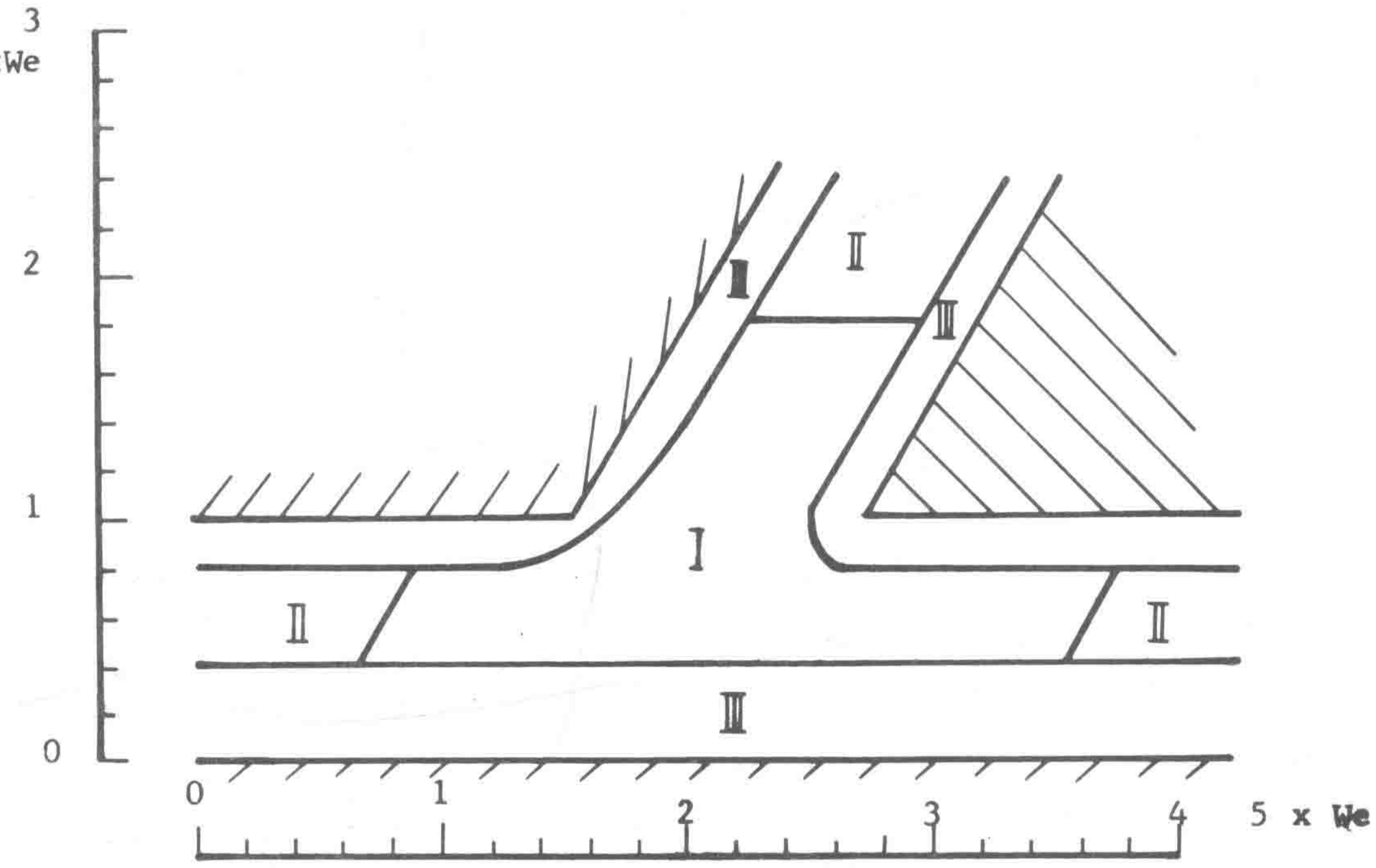

REGION	BOLT LENGTH	REQUIRED SHEAR RESISTANCE	REQUIRED PRETENSION
I	l_b	Sr	P
II	0.8 l_b	0.5 Sr	0.5 P
III	0.6 l_b	0.3 Sr	0.3 P

Fig. 23 The Proposed Bolting Pattern for Reinforced Method

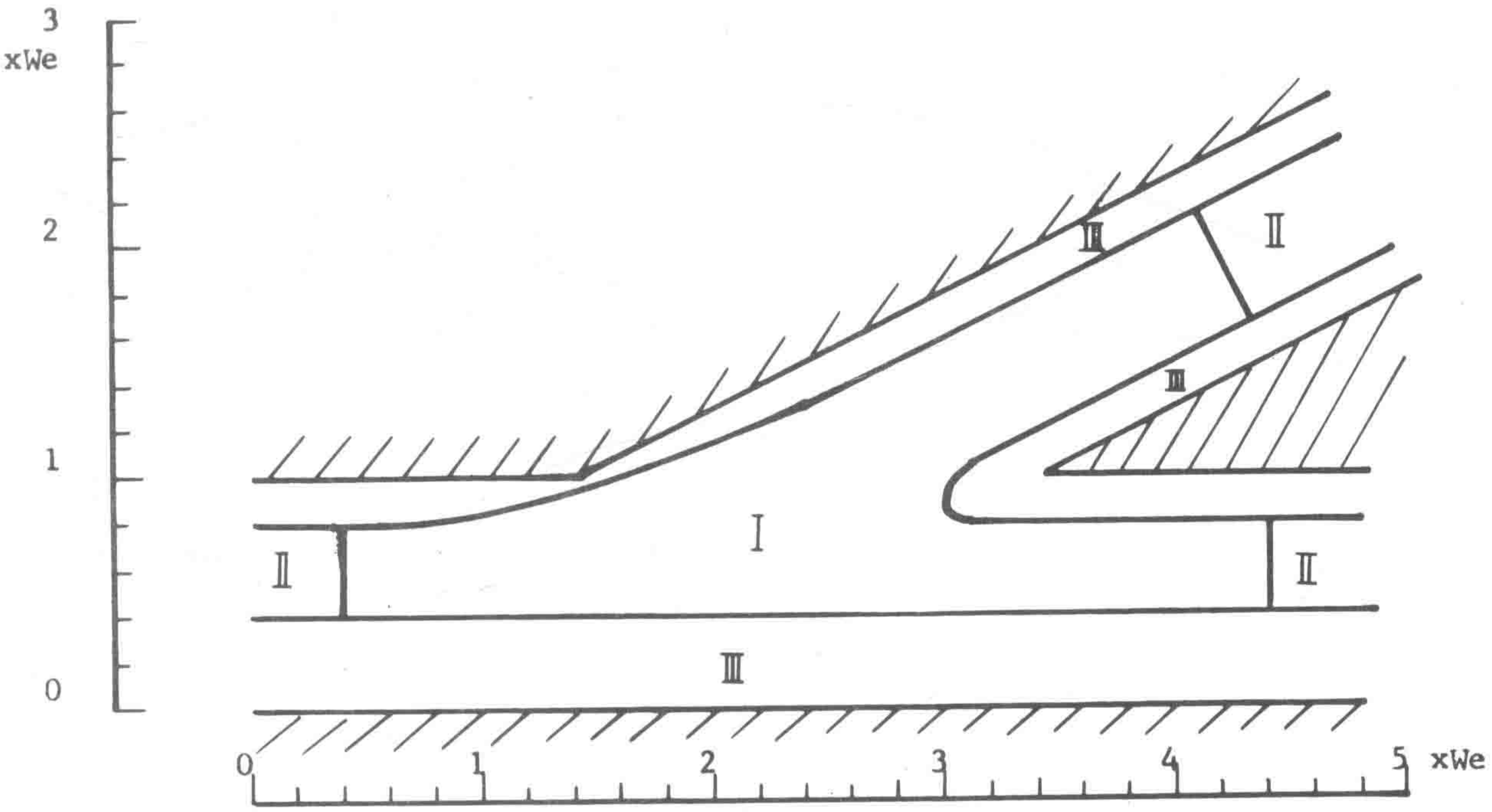

REGION	BOLT LENGTH	REQUIRED SHEAR RESISTANCE	REQUIRED PRETENSION
Ⅰ	l_b	Sr	P
Ⅱ	0.8 l_b	0.4 Sr	0.4 P
Ⅲ	0.6 l_b	0.2 Sr	0.2 P

Fig. 24 The Proposed Bolting Pattern for Reinforced Method